SCHOOL OF ADVANCED STUDIES OF THE ROMANIAN ACADEMY
DOCTORAL SCHOOL OF CHEMICAL SCIENCES
„PETRU PONI" INSTITUTE OF MACROMOLECULAR CHEMISTRY IAȘI
Doctoral domain CHEMISTRY

INTELLIGENT SYSTEMS DESIGNED FOR THE TRANSPORT OF ACTIVE CHEMICAL SPECIES. OBTAINING. CHARACTERIZATION
DOCTORAL THESIS SUMMARY

Doctoral supervisor:
DR. PINTEALĂ MARIANA

PhD student:
COȘEREANU (căs. ZONDA) RADU

2024

TABLE OF CONTENTS

INTRODUCTION

In recent decades, nanotechnology has revolutionized the way chemical transport is approached. Nanoparticles and nanosystems can be designed and programmed to deliver specific molecules to precise sites in the body. In the field of gene therapy and genetic engineering, delivery systems have advanced considerably to enable precise delivery of genes and proteins to target cells. With the advancement of computer technologies and artificial intelligence, intelligent transportation systems have been developed that can monitor and control the delivery of chemicals in real time.

Smart transport systems for active chemical species in a biological environment are essential in the medical field, enabling precise drug delivery and application of therapies, reducing side effects and improving treatments. In biotechnology and genetic engineering, these systems facilitate the precise delivery and integration of genes and proteins, with the potential to revolutionize gene therapies. In addition, they can be used in diagnostics, increasing the speed and accuracy of diagnostics, and in protecting the environment, detecting and eliminating chemical pollution. In conclusion, intelligent transport systems for active chemical species bring numerous benefits, including improving medical treatments, advancing genetic engineering, accurate medical diagnosis, protecting the environment, and significant savings, and represent a vital tool in scientific and medical fields with significant potential in advancing knowledge and improving life. This desiderate allows the implementation of new innovative functional structures necessary to perfect the methods of targeted administration of active principles by means of specific biological markers.

In this context, the research theme addressed in this doctoral thesis, ***"Intelligent systems designed for the transport of active chemical species. Obtaining. Characterization"***, falls within the current research trends through the development of supramolecular ion channel type systems for the transport of cations through natural or artificial membranes. The thesis also aimed to address the identification of a specific marker for early neonatal sepsis in order to subsequently design a system for the release of active principles at the affected sites, identified with the help of the marker.

The doctoral thesis benefited from funding through the ***ORIZONT 2020*** international project***, „SupraChem Lab - Laboratory of Supramolecular Chemistry for Adaptive Delivery Systems - ERA Chair initiative"***, implemented within the Advanced Research Center for Bionanoconjugates and Biopolymers, from the "Petru Poni" Institute of Macromolecular Chemistry in Iași.

The mentioned project aimed to promote excellence in research by establishing a group specialized in the design, synthesis and characterization of adaptive self-organized supramolecular structures. In this context, a research subgroup addressed the development of dynamic interactive systems used in the formation of water and ion channels with the help of small molecular compounds able to self-assemble into functional supramolecular structures inside lipid bilayer membranes.

The subject of the thesis corresponds to the research theme of this project, aiming at the integration of the study of artificial ion channels obtained by dynamic supramolecular organization, in intelligent transport systems. These systems are able to perform complex functions in a biological assembly, leading to the development of new procedures for the controlled release of active principles.

The research integrated in the PhD thesis pursues the idea of transporting active principles embedded in liposomes and releasing them at a target point. The advantage of using liposomal systems in studying the transport of active species in the biological environment lies in the similarity of their membrane with the cell membrane. In this sense, in the doctoral thesis, strategies were developed for the creation of ion channels, through the self-assembly of small molecular compounds, in the liposomal membrane and the identification of endocan as a biomarker in sepsis in newborns.

For the formation of self-assembled supramolecular structures in the liposomal membrane, derivatives of crown ethers capable of forming ion channel-type supramolecular structures through hydrogen bridges or π-π interactions ensured by the functions attached to the crown ether were studied. Experimental methods based on ion transport through liposomal membranes and theoretical computer calculation methods were used to evaluate the transport capacity.

The doctoral thesis is divided into *two sections*. The **first section** is an overview of liposome-based transport systems and the opportunity of their application in the targeted transport of active species, and the **second section** of the thesis presents our results on the experiments carried out both to evaluate the transport capacity of the studied crown ether derivatives, as well as investigating the possibility of using endocan as a biomarker in sepsis in newborns.

To evaluate ion transport through lipid membranes, the HPTS method was used, which involves the use of fluorescence spectroscopy, using large unilamellar vesicles (100 μm) with bilayer lipid membranes (liposomes) and a pH-sensitive fluorophore, 8-hydroxypyrene- 1, 3, 6 – sodium trisulfonate (HPTS). The method consists of introducing the fluorophore inside the

vesicle to detect pH changes due to ion transport across the membrane. Through this procedure, the self-assembly of alkyl-benzoureido-ether-crown compounds was investigated by means of hydrogen bridges, with the formation of ion channels inside the liposomal membrane. Through HPTS tests, the existence of ion transport was observed, and molecular dynamics calculations suggested a "carrier" type transport process due to the translation of crown alkyl-benzoureido-ether molecules from one face to the other of the lipid membrane.

The possibility of self-assembly in environments with different polarities of two 18-crown-6 ether derivatives functionalized with pyrene groups symmetrically linked via imine and azo groups was also explored. The experimental results obtained by UV-vis absorption, fluorescence and WAXD were correlated with ground-state quantum mechanical and molecular dynamics computer calculations. After corroborating the experimental and theoretical results, it was observed that the two compounds are able to form pyrene "stacks", more ordered or less ordered depending on the polarity of the environment or the organic sequence through which the attachment of the pyrene units was achieved. Thus, if the pyrene groups were attached to the crown ether through imine bonds, "stacks" composed of only 2-3 molecules are formed, while when the pyrene groups were attached through -N=N- (azo) bonds, a planar geometry of the molecule, a fact that favors the formation of ordered pyrene "stacks" composed of a significant number of molecules.

The investigation of endocan as a potential biomarker in early neonatal sepsis is a prospective study of its further use as a target in the design of intelligent delivery systems of active principles in combating sepsis. From the studies carried out in this chapter, the conclusion can be drawn that endocan can be considered a useful marker in the diagnosis of early neonatal sepsis, as well as in the follow-up of the evolution under treatment.

The information extracted by this PhD thesis involved complex interdisciplinary studies in fields such as supramolecular chemistry, physics, physical chemistry, computer computation, biology, biochemistry and medicine. These represent models for further development of transport systems through synthetic ion channels created in liposomal membranes.

PART II

ORIGINAL CONTRIBUTIONS

CHAPTER 3. BIOMIMETIC SUPRAMOLECULAR ASSEMBLIES FOR ION TRANSPORT THROUGH LIPID MEMBRANES

General objective: Preparation and characterization of ion channels by self-assembly in lipid membranes based on phosphatidylcholine;

Specific objectives:

- Preparation of ion channels based on benzo-ether-crown monofunctionalized with alkyl-urea groups;
- Preparation of ion channels based on crown dibenzo-ethers symmetrically functionalized with azo-pyrene or imino-pyrene groups.

3.1. Introduction - Crown ethers and ion transport

Crown ethers are macrocyclic polyether organic compounds, meaning they are made up of multiple ether groups [1]. The most common crown ethers are cyclic oligomers of ethylene oxide, the repeating unit in the molecule being the ethyleneoxy residue [2], –$[CH_2CH_2O]_n$–. The most important representatives of this class of compounds are the tetramer ($n = 4$), pentamer ($n = 5$), hexamer ($n = 6$) and heptamer ($n=7$), formulas also highlighted in Figure 3.1.
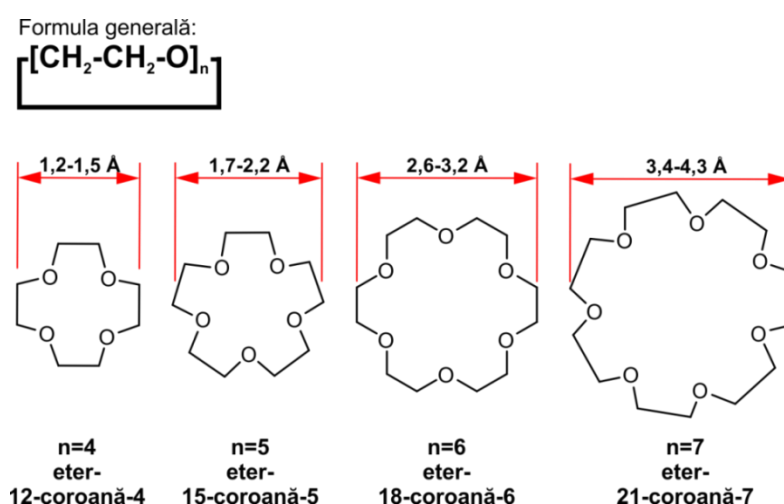
Figure 3.1. Sizes and chemical structures of the most widely used crown ethers (adapted from ref [3])

It is well known in the literature that crown ethers form complexes with alkali metal ions, the affinity between them being mainly determined by the ionic radius corroborated with the ring size of the crown ether (Figure 3.2) [3–5].
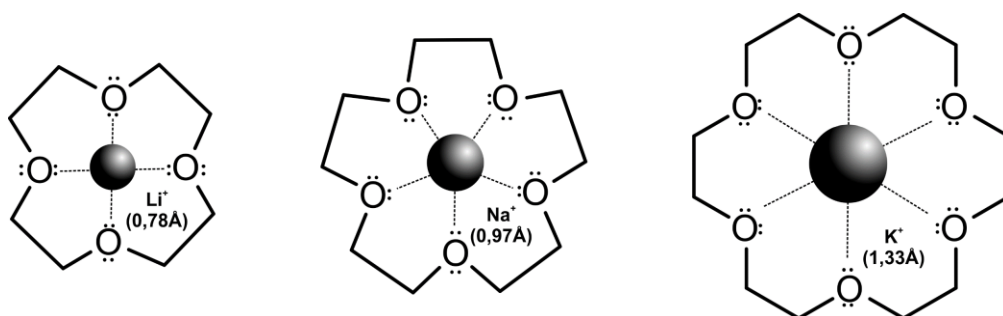
Figure 3.2. Complexes of alkali metals with crown ethers (adapted from ref [5])

The ability of crown ethers to selectively interact with alkaline ions can be used in the construction of ion channels, components in the structure of double-layer lipid membranes. For a compound to form ion channels by self-assembly in bilayer lipid membranes, it must cumulatively meet several criteria (Figure 3.3):

1. To be able to form intermolecular bonds – for self-assembly
2. To interact with transported ions – for selectivity
3. To present a hydrophobic part - for integration into the lipid layer
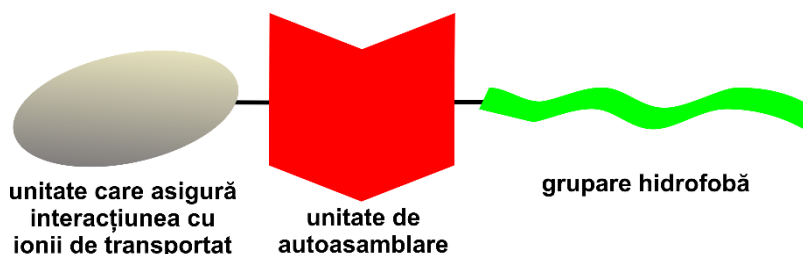
Figure 3.3. The components necessary for a molecule to form supramolecular structures capable of performing the function of ion channels

3.2. Self-assembly in the lipid membrane by hydrogen bonds of crown benzoethers monofunctionalized with urea alkyl groups

3.2.1. Design and synthesis of synthesized compounds

In this study we investigated the hydrogen-bonding self-assembly and ion transport capacity of alkyl-benzoureido-ether-crown compounds across the phosphatidylcholine liposomal membrane. The structure of the compounds synthesized for this purpose is presented in Scheme 3.1.
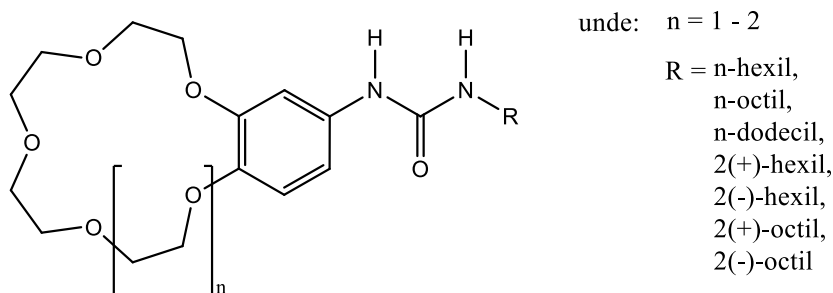
Scheme 3.1. General structure of synthesized compounds of type

alkyl-benzoureido-ether-crown.

The synthesized compounds present three characteristic sites: (a) the crown ether, which provides ionic transport; (b) the hydrophobic group, represented by the linear or branched alkyl radical; (c) the group capable of forming intermolecular hydrogen bridges, represented by the urea group [6]. Scheme 3.2 shows the principle of aggregation of crown benzoureido-ether units in supramolecular structures, and Scheme 3.3 shows the reaction to obtain the studied alkyl-benzoureido-crown ethers.
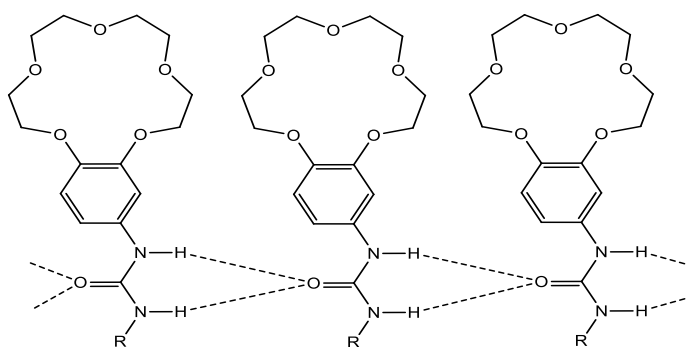
Scheme 3.2. Principle of aggregation of benzoureido-ether-crown units

in supramolecular structures (adapted from refs [6,7])
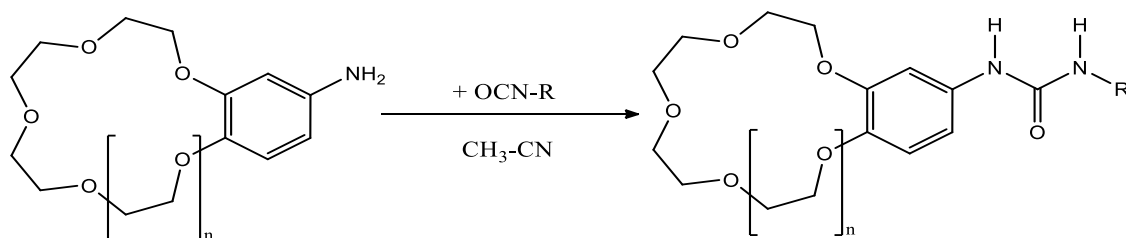
Scheme 3.3. Obtaining the studied alkyl-benzoureido-crown ethers, where n and R can be

found in Table 3.1.

9

3.2.2.2. Synthesis of crown benzoethers functionalized with alkyl-urea groups

For the preparation of alkyl-benzoureido-crown ether compounds, 50 mg of amino-benzo-ether-15-crown-5 were dissolved in 2 mL of acetonitrile, over which 1.1 volumes of alkyl isocyanate were added to obtain the required compound, according to Table 3.1. The reaction mixture was refluxed for 24 hours. All operations were performed under dry nitrogen atmosphere. After refluxing, the reaction mixture was kept at -20 °C for 24 h, then rapidly filtered. The precipitate was dried under vacuum for 3 days.

Table 3.1. The alkyl residues (R) and the size of the crown ether (n) corresponding to the synthesized compounds (Scheme 3.3.).

	R	n	Compound name	Compound code	Theoretical molecular mass
1	butyl	1	Butyl-benzoureido-ether-15-crown-5	15c5C4	382,45
2	hexyl	1	Hexyl-benzoureido-ether-15-crown-5	15c5C6	410,50
3	hexyl	2	Hexyl-benzoureido-ether-18-crown-6	18c6C6	454,56
4	octyl	1	Octyl-benzoureido-ether-15-crown-5	15c5C8	438,56
5	dodecyl	1	Dodecyl-benzoureido-ether-15-crown-5	15c5C12	494,66
6	(s)-(+)-2-hexyl	1	(s)-(+)-2-hexyl-benzoureido-ether-15-crown-5	15c5C6+	410,50
7	(r)-(-)-2-hexyl	1	(r)-(-)-2-hexyl-benzoureido-ether-15-crown-5	15c5C6-	410,50
8	(s)-(+)-2-octyl	1	(s)-(+)-2-octyl-benzoureido-ether-15-crown-5	15c5C8+	438,56
9	(r)-(-)-2-octyl	1	(r)-(-)-2-octyl-benzoureido-ether-15-crown-5	15c5C8-	438,56

3.2.2.3. Structural characterization of crown benzoether compounds functionalized with alkyl-urea groups

^{1}H-NMR spectra were recorded in dimethyl sulfoxide-d6 (DMSO-d6) using a DRX 300 MHz spectrometer (Bruker Scientific Instruments, Billerica, MA USA), and electrospray ionization mass spectrometry (ESI-MS) analysis of was performed to confirm the structure of the synthesized compounds using the Agilent 6500 Series Accurate-Mass Quadrupole Time-of-Flight (Q-TOF) LC/MS system (Agilent Technologies, Inc., Santa Clara, CA USA).

3.2.2.4. Preparation of phosphatidylcholine-based liposomes loaded with sodium 8-hydroxypyrene-1,3,6-trisulfonate (HPTS)

Liposomes were obtained by solubilizing L-α-phosphatidylcholine (EYPC) in organic solvent, followed by evaporation of the organic solvent and obtaining a film of L-α-phosphatidylcholine. This was then hydrated by manual agitation with a phosphate buffered saline solution (PBS, pH=6.5) containing sodium 8-hydroxypyrene-1,3,6-trisulfonate (HPTS). After the film was completely dispersed in the aqueous solution, the resulting solution was subjected to rapid successive freeze/thaw cycles followed by extrusion using an extruder fitted with a 100 nm pore diameter filter. The obtained vesicles were purified by passing through a column of Dextran G-50 and washing the liposomes with PBS to remove HPTS from the external environment [8].
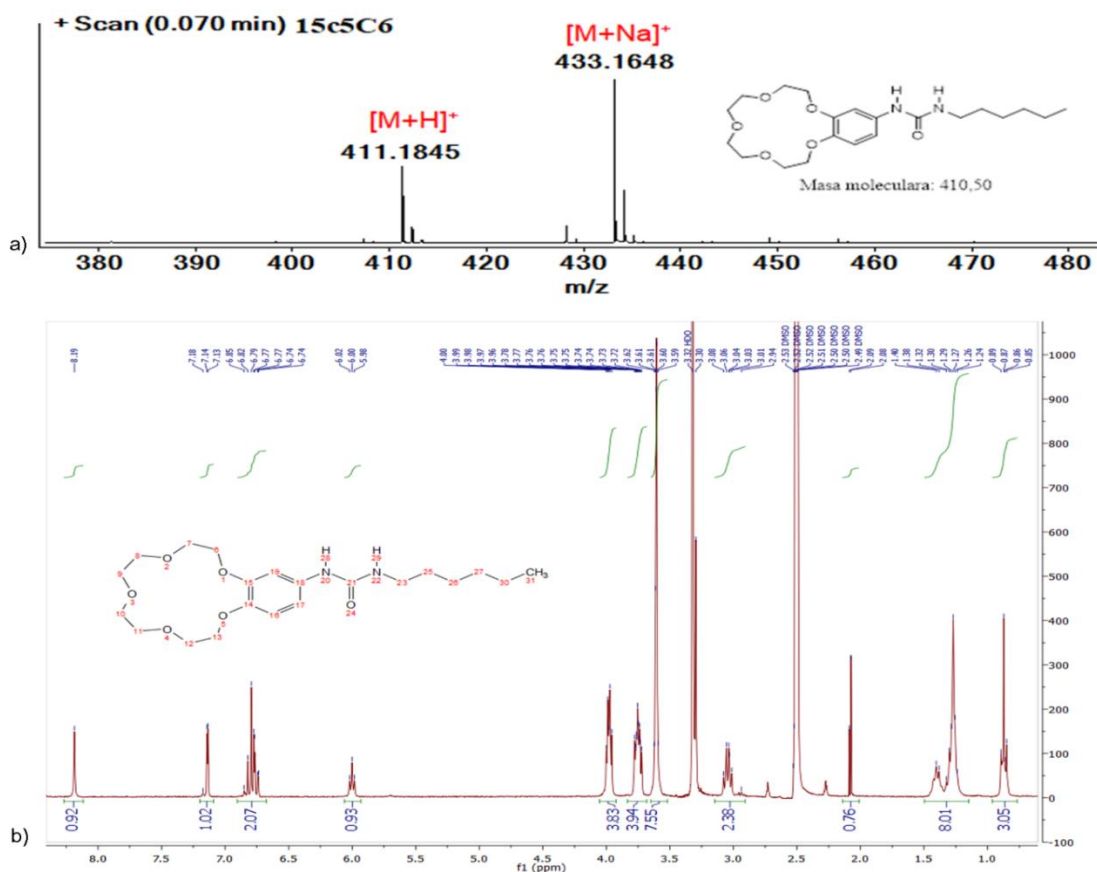
Figure 3.5. Mass spectrum (a) and ^{1}H-RMN spectrum (b) for compound 15c5C6. ESI-MS: m/z [M+H]$^+$ = 411,18 [M+Na]$^+$ = 433,16. ^{1}H-NMR: ((CD$_3$)$_2$S=O, ppm) δ = 0.86 (t, 3H, **CH$_3$**), 1.26 (m, 8H, **CH$_2$**), 3.03 (m, 2H, **CH$_2$**), 3.59 (m, 8H, -O-**CH$_2$-CH$_2$** –O crown ether), 3.74 (m, 4H, -O-**CH$_2$-CH$_2$**-O- crown ether), 3.97 (m, 4H, -O-**CH$_2$-CH$_2$**-O- crown ether), 6.00 (t, 1H, N**H**-Alkyl), 6.79 (m, 2H, **H**-Ar), 7.13 (d, 1H, **H**-Ar), 8.19 (s, 1H, N**H** -Ar).

3.2.3.1. Analysis of the selective transport capacity of alkaline cations of alkyl-benzoureido-crown ethers through the liposomal membrane using the HPTS method

The transport capacity of alkaline cations: Li^+, Na^+, K^+, Rb^+ and Cs^+ through liposomal membranes of all synthesized compounds was achieved by the HPTS method as we can see in Figures 3.13 and 3.19.
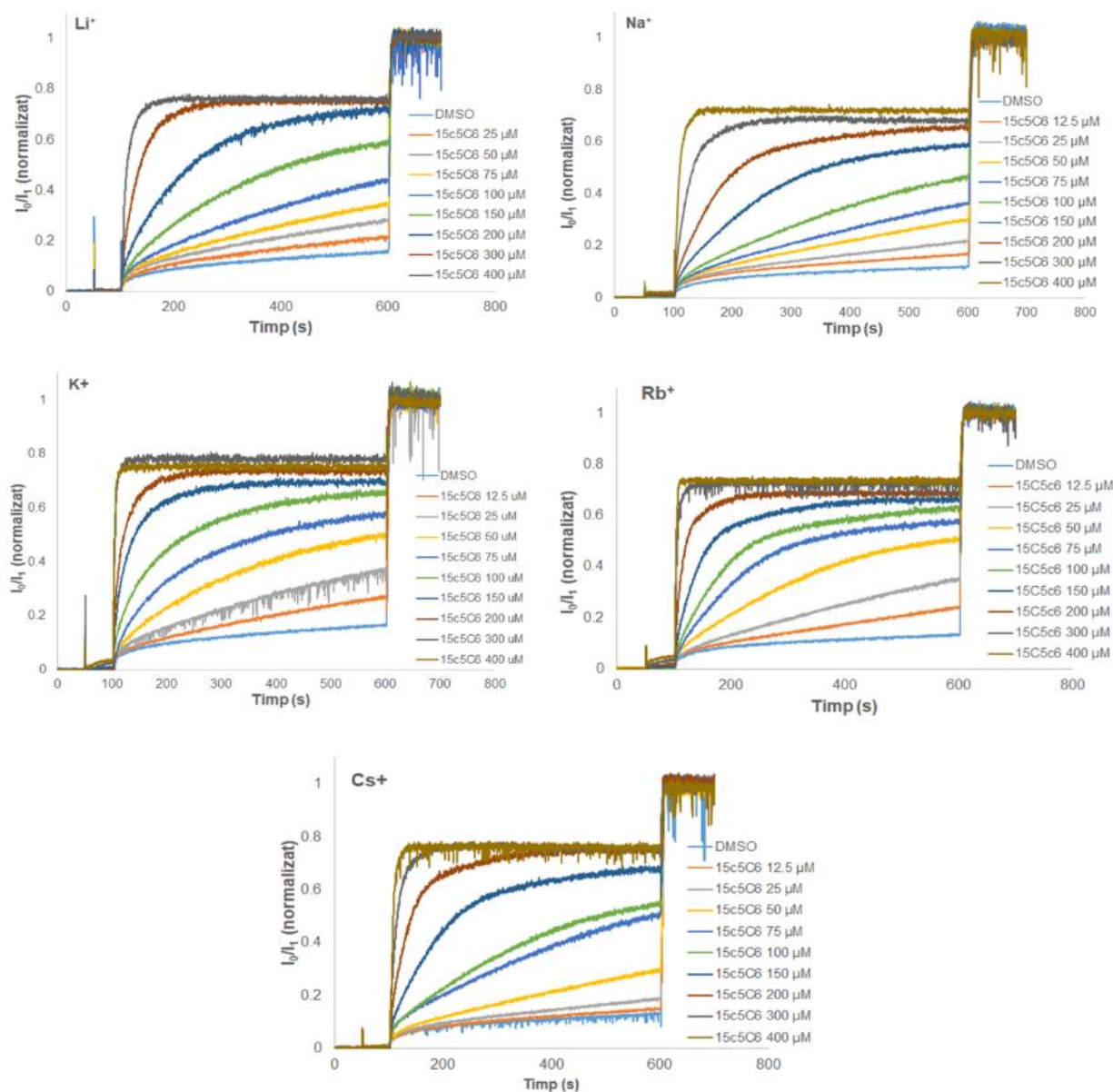
Figure 3.13. Variation of normalized I_0/I_1 values vs. time due to the transport of Li^+, Na^+, K^+, Rb^+ and Cs^+ ions as a function of the concentration of compound 15c5C6 in the liposomal membrane.
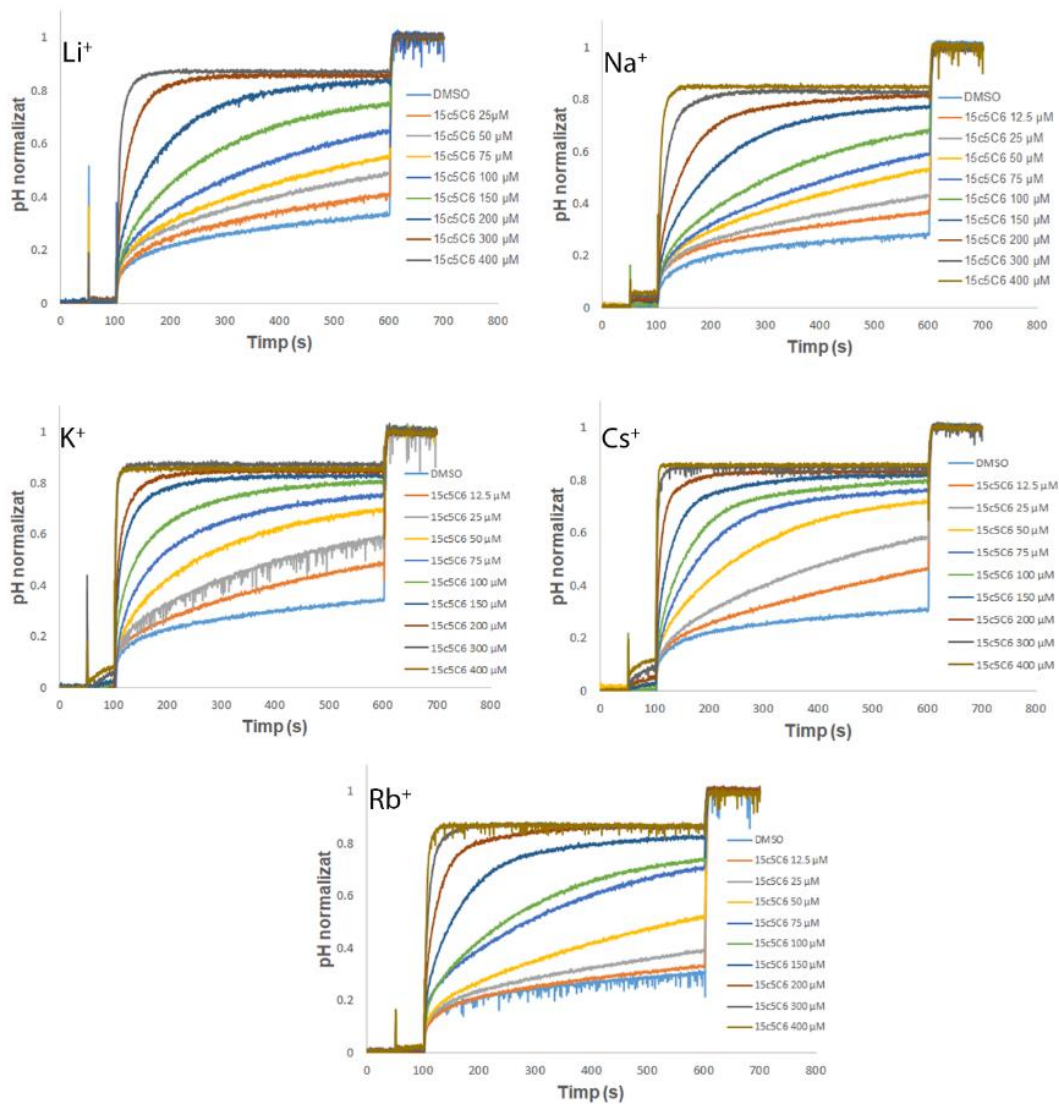
Figure 3.19. Variation of normalized pH values vs. time due to the transport of Li$^+$, Na$^+$, K$^+$, Rb$^+$ and Cs$^+$ ions as a function of the concentration of compound 15c5C6 in the liposomal membrane.

Table 3.3. Ion transport rate (k), fractional activity (Y), effective concentration (EC_{50}) and Hill coefficient (n) values calculated for compound 15c5C6

	Final concentration (µM) of the studied compound	Li^+	Na^+	K^+	Rb^+	Cs^+
$k\ (s^{-1})$	0	0,025	0,0115	0,0272	0,0325	0,0172
	12,5	-	0,0144	0,0279	0,0221	0,0219
	25	0,0339	0,0183	0,0382	0,0266	0,015
	50	0,025	0,0167	0,0315	0,0472	0,0144
	100	0,0349	0,0269	0,1088	0,0557	0,0193
	200	0,0375	0,0289	0,0626	0,0724	0,0377
	300	0,0448	0,0342	0,1066	0,1033	0,0428
	400	0,0464	0,052	0,1285	0,1656	0,076
$Y\ (u.a.)$	0	0,0935	0,1608	0,3526	0,3543	0,0917
	25	0,2081	0,3007	0,5682	0,6010	0,2560
	50	0,3075	0,4045	0,7106	0,7204	0,5806
	75	0,4604	0,5653	0,8544	0,7842	0,6404
	100	0,7047	0,7844	0,9210	0,8588	0,8469
	200	0,9953	0,9308	1,0949	0,9563	0,9987
	300	1,0000	1,0000	1,0000	1,0000	1,0000
	400	0,0935	0,1608	0,3526	0,3543	0,0917
EC_{50} (µM)		78,66	71,15	36,14	37,95	0,01
n (u.a.)		2,89	1,66	1,59	1,42	2,13

Molecular dynamics simulations (DM)

For a better understanding of the mechanism of ion transport through lipid membranes, an atomistic dynamic simulation was used for a time interval of 500 ns. The studied molecules have the crown ether depicted in blue, and the alkyl end in yellow, lipids are represented by fine turquoise lines, and water molecules by red spheres. All studied crown ethers form complexes with Na^+ and K^+, as can also be seen in Figure 3.38.
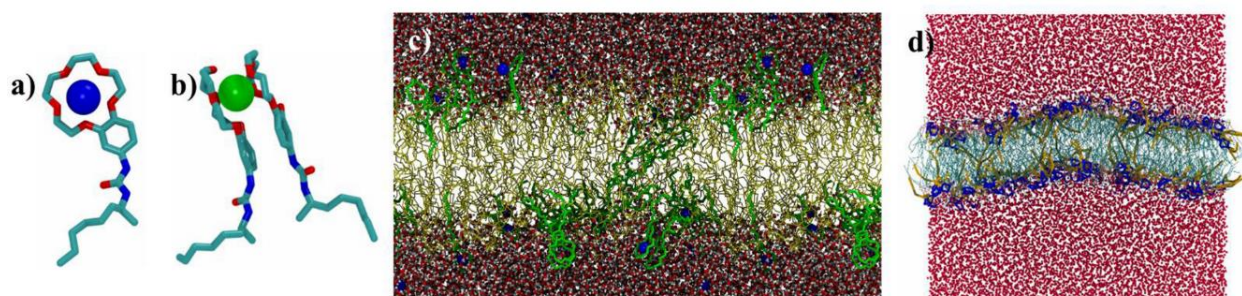
Figure 3.38. Atomistic computer simulation of a) Na^+ and b) K^+ cation transport mediated by compound 15c5C8+. c) Cross-section through the liposomal membrane in the atomistic simulation of Na^+ transport in the presence of the compound 15c5C8+. d) Cross-section through the liposomal membrane in the Course-Grain simulation of Na^+ transport in the presence of the compound 15c5C8+ (adapted from ref [9])

The main difference between the complexes of the two alkali metals is the number of crown ethers coordinated by the cations, Na^+ thus forming much more stable complexes with a single crown ether while K^+ causes the formation of complexes with two crown ether molecules. In any case, both structures were found for a very short time in both Na^+ and K^+ - based complexes. Moreover, in the case of the compound 15c5C8+, a formation of crown ethers crossing the lipid membrane was observed for a short period (Figure 3.38.c).

Also, the Course-Grain (CG) model allowed us to extend the simulation time to 10 μs. This model also did not reveal a stable formation over time (Figure 3.38.d) during the simulation period, possibly due to the instability of the formed channel. During the CG simulation a few molecules of crown ether derivatives were observed to act according to the "flip-flop" pattern, suggesting a "carrier" type transport mechanism (Figure 3.38.d). All these observations suggest a complex mode of transport, a combination of the dynamic constitution of some ion channels, on the one hand, and of the "carrier" type, on the other hand, these conclusions being in accordance with the experimental results.

3.2.4. Conclusions

- ❖ For all the compounds studied and presented in this chapter, increasing their concentration causes an increase in the rate of transport of cations through the membrane by them.
- ❖ Following the analysis of EC_{50} and k, it was observed that ion transport through the membrane is more efficient in the case of the compounds with the longer alkyl chain

(15c5C8 and 15c5C12) compared to the compound with the shorter alkyl chain, 15c5C6.

❖ Differences are observed between the transport mediated by 15c5C8 and 15c5C12 depending on the ion transported by them. Thus, K^+ transport is faster and more efficient when using 15c5C12.

❖ By replacing the linear alkyl radical with an optically active branched one, no notable differences in selectivity were recorded, the transport activity of compounds with optically active octyl being intermediate to those with n-hexyl and respectively n-octyl.

❖ For all studied compounds, the highest activity is found in the transport of K^+ and Rb^+ ions, and the lowest transport activity corresponds to the ions with the smallest radii, Li^+ and K^+, a situation highlighted by the values of the fractional activity Y and supported by k and EC^{50} values.

❖ During the DM simulations, the self-assembly of the compounds into stable ion channels was not observed, but in the Course-Grain simulation, the translation of crown alkyl-benzoureido-ether molecules from one face to the other of the lipid membrane was observed, which can suggest the existence of a "carrier" transport process.

❖ The results obtained so far suggest a complex transport mechanism, for which further detailed study is necessary.

3.3. Functionalized crown ethers with self-assembly properties through $\pi - \pi$ interactions in media with different polarities for the transport of alkali cations

A particular way to create supramolecular structures is the use of π-conjugated molecules. For this purpose, pyrene is a good choice due to its propensity to self-aggregate through $\pi - \pi$ stacking, a phenomenon that can be detected with the help of fluorescence spectroscopy [10,11]. Since the pyrene units can be self-assembled by the π–π stacking interaction in the ground state and the excited state, the photophysical properties change continuously so that the fluorescence emission can be enhanced or quenched [12,13].

3.3.2. Study of supramolecular arrangements of di-iminopyrene-dibenzo-ether-18-crown-6 derivatives

Objective*:* Synthesis, structural characterization and investigation of self-assembly properties in media with different polarities of di-iminopyrene-dibenzo-ether-18-crown-6.

This chapter presents the synthesis of di-iminopyrene-dibenzo-ether-18-crown-6 (named DPyDB–C=N–18C6), which is a new compound that includes the crown ether and the pyrene moieties linked by –HC=N– bonds in symmetrical to the etheric cycle (Figure 3.39.).
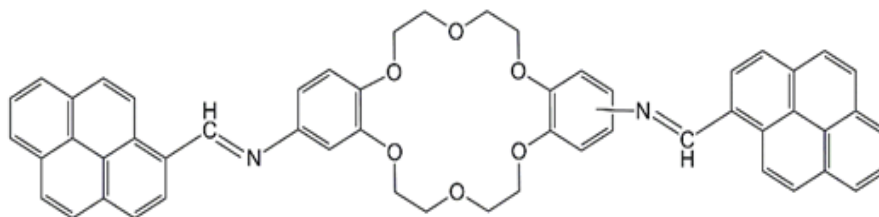
Figure 3.39. Structural formula of di-iminopyrene-dibenzo-ether-18-crown-6 (adapted from ref [13])

The aim of the present study was to demonstrate the formation of a potential supramolecular arrangement mediated by inter- and intramolecular interactions between DPyDB–C=N–18C6 molecules.

Synthesis of di-iminopyrene-dibenzo-ether-18-crown-6 (DPyDB-C=N-18C6)

To a solution of 18-crown-6-diaminodibenzoether (200 mg, 0.51 mmol) in ethanol (20 mL), was added acetic acid (200 µL, 2.80 mmol, 4 equiv) and 1 -pyrenecarboxaldehyde (260 mg, 1.15 mmol, 2.1 equiv.). The resulting mixture was stirred at room temperature for 24 h, filtered and purified by centrifugation from dichloromethane and ethyl ether. A yellow solid product was obtained in 80% yield.

3.3.2.3. Results and discussion

Synthesis and physicochemical characterization of di-iminopyrene-dibenzo-ether-18-crown-6 (DPyDB-C=N-18C6)

DPyDB-C=N-18C6 was prepared by the direct reaction between the amine groups of diaminodibenzoether-18-crown-6 and the aldehyde group of 1-pyrenecarboxaldehyde, in acidic medium, with the formation of imine bonds between the two precursors, as are presented in Scheme 3.4. Diaminodibenzo-ether-18-crown-6 was synthesized as described by Ardeleanu et al. [14], as a mixture of two positional isomers (denoted as i1 and i2) with respect to the position of the amino group attached to the phenyl ring.
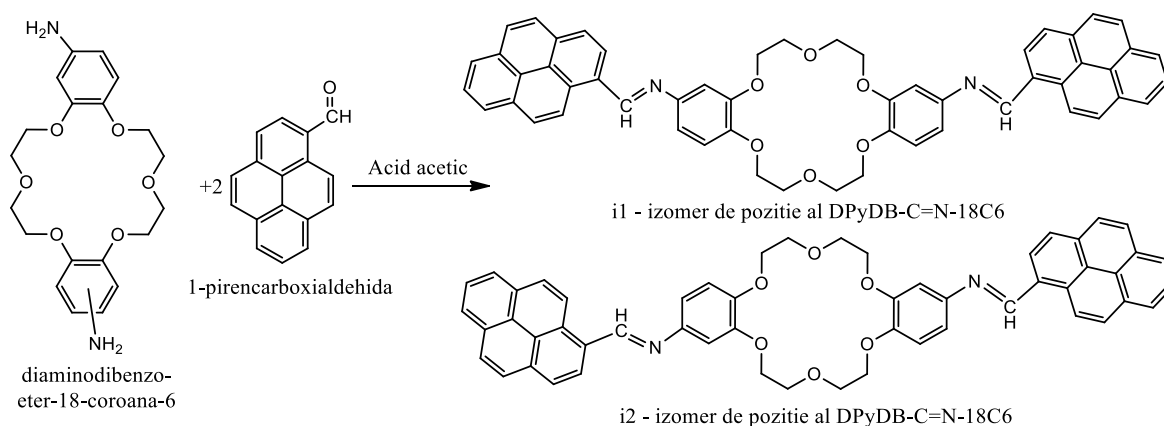
Scheme 3.4. Synthesis method of the compound DPyDB-C=N-18C6 (adapted from ref [13])
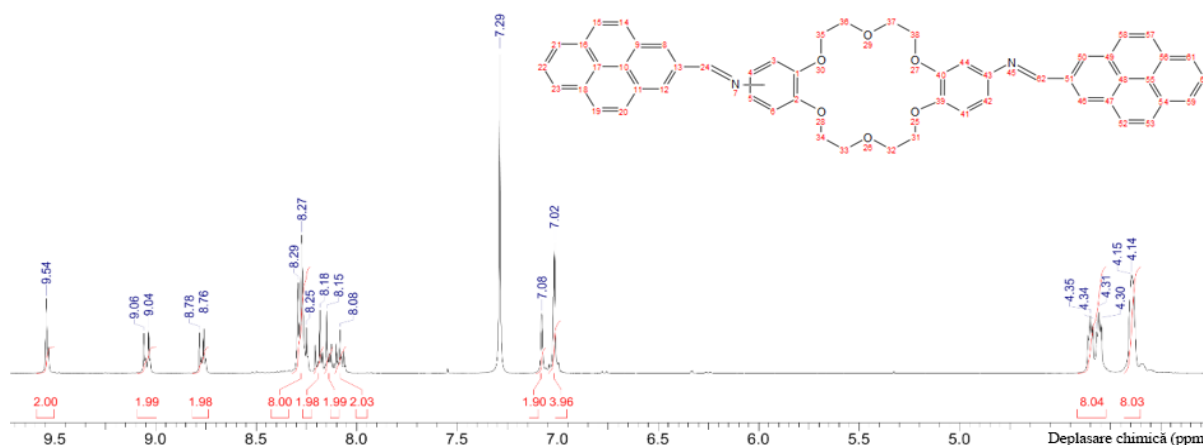
Figure 3.41. ^{1}H-RMN spectrum for compound DPyDB–C=N–18C6. ^{1}H-RMN (400 MHz, CDCl$_3$): δ = 4,14 (as, 8H), 4,35 (dd, 8H), 7,02 (d, 4H), 7,08 (s, 2H), 8,08 (d, 2H), 8,15 (d, 2H), 8,18 (d, 2H), 8,28 (m, 8H), 8,77 (d, 2H), 9,05 (d, 2H), 9,54 (s, 2H) (adapted from ref [13])

Molecular dynamics simulations (DM)

To investigate the aggregation ability of the compound di-iminopyrene-dibenzo-ether-18-crown-6, DM simulations of the aggregation process in ethanol were performed. Both positional isomers were included in the DM simulations, so Figure 3.47 shows the initial conformation of the compounds of the system. In yellowish green is the **i1**-position isomer and in green is the **i2**-position isomer.

18
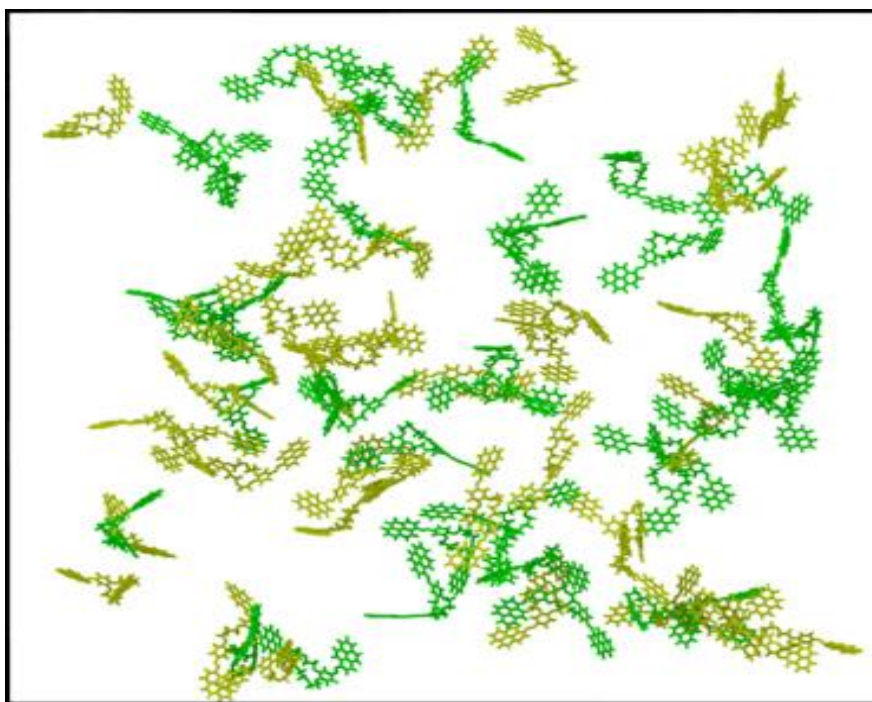
Figure 3.47. The initial structures of the compound DPyDB–C=N–18C6 after energy minimization (adapted from ref [13])

For the molecular simulation under high concentration conditions, 23,278 solvent molecules and 40 molecules of each positional isomer were introduced into the simulation cell, resulting in a single aggregate capable of highlighting the intermolecular interactions that govern the aggregation process and can reach equilibrium in a reasonable simulation time (800 ns). Figure 3.48.a illustrates the final structure of the aggregate DPyDB–C=N–18C6.
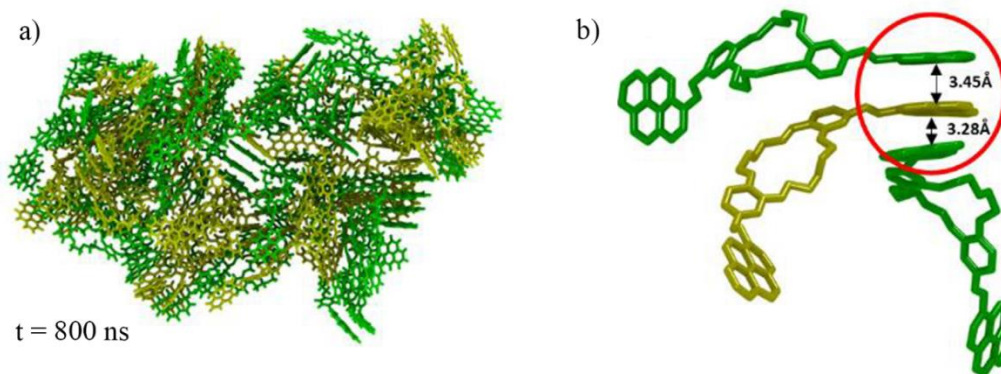
Figure 3.48. a) The final structure of the DPyDB–C=N–18C6 aggregate, obtained after 800 ns of simulation; **b)** Detail representing the pyrene-pyrene intermolecular interaction on a single side group (circled in red) (adapted from ref [13])

The visual analysis of the simulated aggregate shows an amorphous structure (Figure 3.48.a), in agreement with the results obtained from the WAXD analysis technique. Despite the high degree of disorder of the aggregate, it can be seen that the pyrene units are able to form intermolecular $\pi - \pi$ stacks between three to four parallel pyrene units originating from different molecules, with interaction distances of about 3.45 and 3.28 Å. The ordered pyrene units develop only on one side of the molecule, the pyrene fragments on the other side being either unaggregated or involved in stacks with pyrene groups belonging to totally different molecules (Figure 3.48.b).

Theoretical studies – quantum mechanics calculations in the ground state

In order to explain the inability of DPyDB–C=N–18C6 to form intermolecular $\pi - \pi$ stacks with the involvement of both pyrene units, we resorted to ground state quantum mechanical calculations.

All equilibrium geometries of both positional isomers (i1 and i2) achieved, after completing the quantum mechanical calculations using the PBE0/6-311+G(d,p) method, are shown in Figure 3.51.
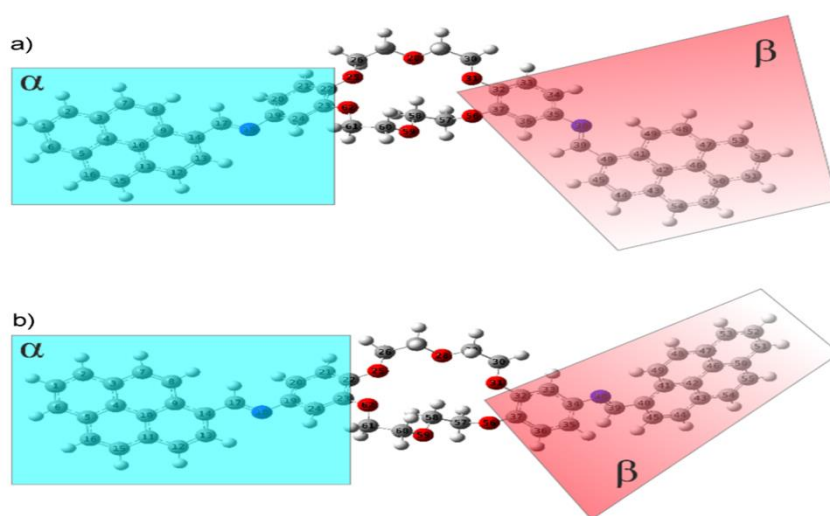
Figure 3.51. Equilibrium geometries in the ground state calculated using the PBE0/6-311+G(d,p) method for: a) isomer **i1**; b) isomer **i2** (adapted from ref [13])

DFT calculations were performed in the ground state, considering the S_0 singlet state as the ground level. The conformational effect was studied by rotating the plane of the pyrene moiety clockwise, while the plane of the phenyl moiety was oriented counterclockwise in small steps of 10°. The conformational effect of the studied compounds was estimated using the potential energy surface (PES).

3.3.2.4. Conclusions

❖ In this chapter, a new compound was synthesized by linking two pyrene fragments to diaminodibenzo-ether-18-crown-6 through imine bonds (–HC=N–), resulting in the product DPyDB–C=N–18C6.

❖ The synthesis was confirmed by FTIR, ^{1}H-NMR, ^{13}C-NMR, TGA and DSC techniques, and the quantitative ^{13}C-NMR analysis revealed the presence of two positional isomers.

❖ It was demonstrated by experimental (WAXD analysis technique) and theoretical (DM simulations) methods that DPyDB-C=N-18C6 forms a supramolecular aggregate with weak $\pi - \pi$ interactions.

❖ DM simulation results showed the existence of almost isoenergetic structures as a light-parallel aggregate with an interaction distance around 3.45 and 3.28 Å.

❖ The experimental and theoretical studies performed showed the formation of small aggregates with weak $\pi - \pi$ interactions and highlighted several aspects that limit the self-assembly capacity of the synthesized molecule, such as the dihedral angle of –C–HC=N–C– twisted by about 40°, leading to the steric repulsion that occurs between the individual molecules.

❖ The photophysical properties of the compound DPyDB–C=N–18C6 in solvents of different polarities (n-hexane, toluene, 1,2-dichloroethane and ethanol) were investigated by UV-vis and fluorescence experiments, as well as by mechanics calculations quantum. The presence of $\pi \rightarrow \pi^*$ and n $\rightarrow \pi^*$ transitions was observed, of which the $\pi \rightarrow \pi^*$ transition due to extended π conjugation was predominant.

❖ Fluorescence analysis showed weak emission which could be explained by photoinduced electron transfer and quenching effects caused by aggregation.

❖ Ground-state frontier molecular orbitals demonstrated that the electron density of DPyDB-C=N-18C6 was localized only on a pyrene-CH=N-phenyl sequence of the crown ether, leading to disruption of the intermolecular $\pi - \pi$ columnar stacking.

3.3.3. Study of supramolecular arrangements of di-azopyrenyl-dibenzo-ether-18-crown-6 derivatives in media with different polarities for the transport of alkali cations

In this chapter we designed a new system based on dibenzo-ether-crown, obtained by modifying the side chain of both amino groups from dibenzo-crown-ether with pyrene fragments, resulting in the formation of two azopyrene groups on each side. The aim of this study was to improve the $\pi - \pi$ stacking ability of the molecules, starting from the hypothesis

that changing the –HC=N– bond, previously reported [13], to the azo bond (–N=N–) would increase the planarity of the molecules.

Synthesis and physicochemical characterization of di-azopyrenyl-dibenzo-ether-18-crown-6 (AzoPy-18C6)

In order to obtain self-assembled supramolecular structures with improved stacking ability, the compound di-azopyrenyl-dibenzo-ether-18-crown-6 (AzoPy-18C6, Scheme 3.5.) was synthesized. AzoPy-18C6 was designed by side chain modifications of both 3,3' amine groups with pyrene moieties, resulting in the formation of two azopyrene groups on either side of the dibenzo-crown-ether. A two-step procedure was applied for the chemical synthesis by reacting the nitroso group of pyrene with the amino groups of 18-crown-6-dibenzo-ether [15–18]. The first step involved the reaction of 1-aminopyrene (1) with potassium peroxymonosulfate (Oxone) at room temperature to obtain 1-nitrosopyrene (2) in high yield (90%). The second step consisted of coupling 1-nitrosopyrene (2) with diamino-dibenzo-ether-18-crown-6 (3) in refluxing acetic acid-toluene for 48 h to yield a mixture of i1 and i2 positional isomers (4a, 4b) of AzoPy-18C6, in a 50:50 ratio, in high yield (82 %).
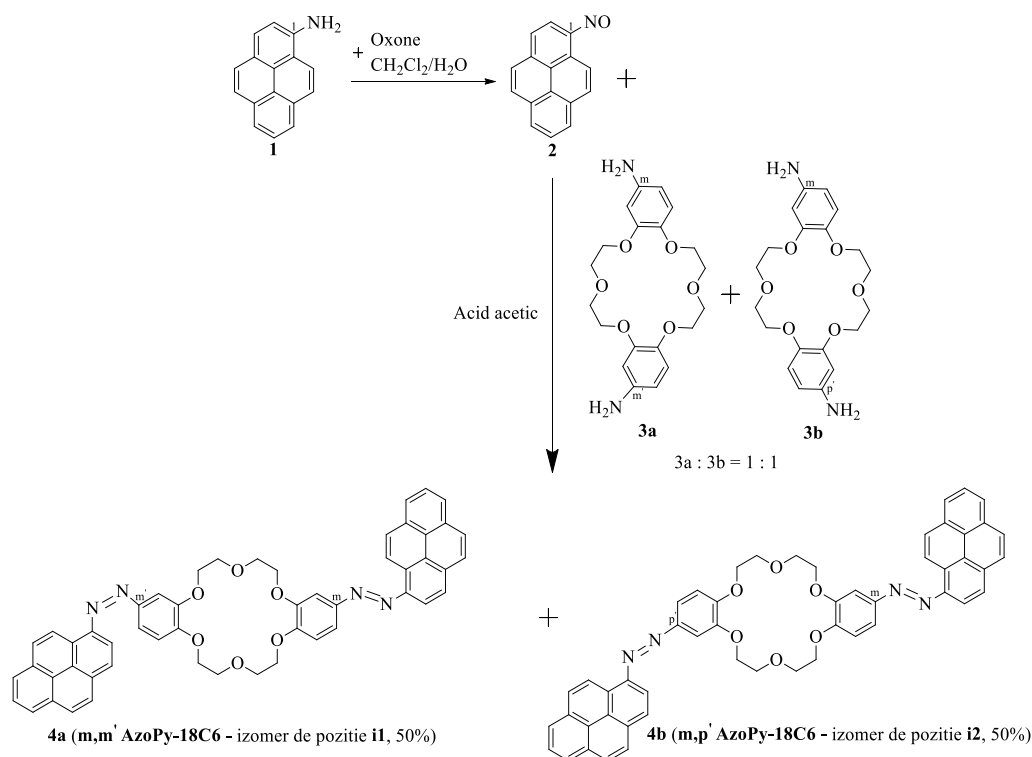
Scheme 3.5. Synthesis scheme for positional isomers 4a (m,m' AzoPy-18C6 - i1) and 4b (m,p' AzoPy-18C6 - i2) in a 50:50 ratio (adapted from ref [19])
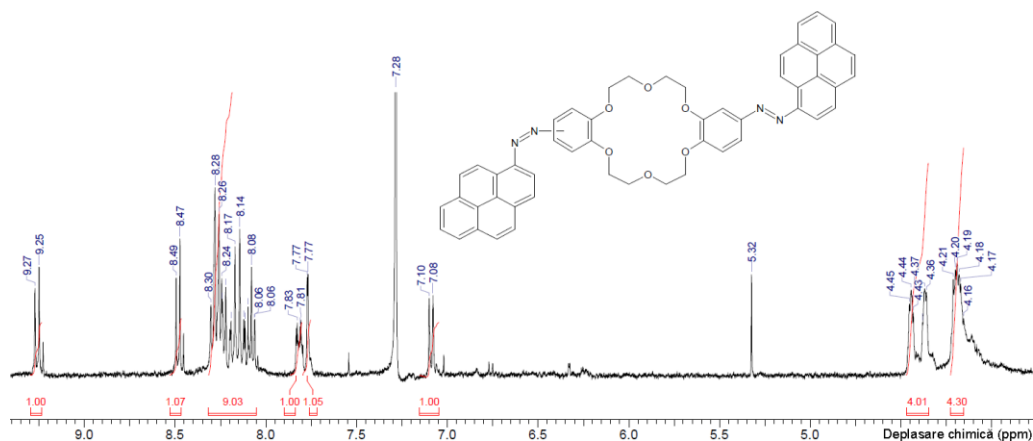
Figure 3.60. ^{1}H-NMR spectrum for compound AzoPy-18C6. *^{1}H-NMR* (400 MHz, CDCl₃): δ = 4,20 (as, 8H), 4,40 (d, 8H), 7,09 (d, 2H), 7,77 (as, 2H), 7,82 (d, 2H), 8,06-8,30 (m, 18H2), 8,48 (d, 2H), 9,26 (d, 2H) (adapted from ref [19])

DM simulations

Since the ^{13}C-NMR spectra showed the presence of two isomers, we performed DM simulations of the aggregation process of the AzoPy-18C6 compound in ethanol to determine the mechanism of the intermolecular interactions and the role of the isomers in these interactions. For the DM simulations, 40 molecules of each positional isomer **i1** and **i2** were used, spread randomly in the simulation box filled with ethanol. Figure 3.65. illustrates the starting locations used: i1-position isomer - green, i2-position isomer - red.
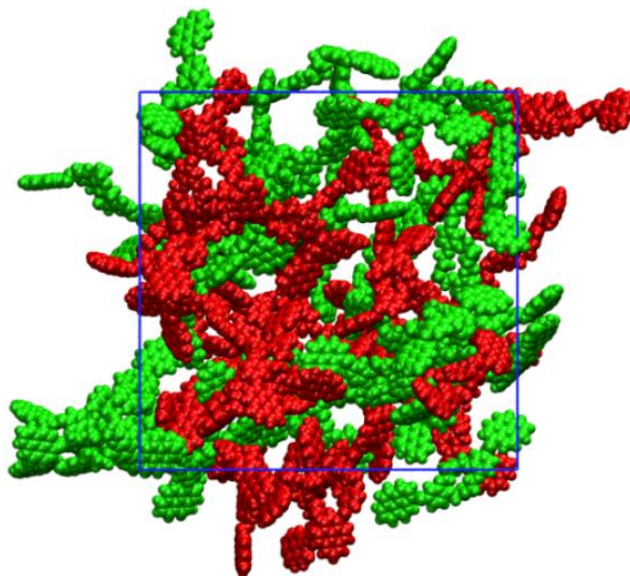
Figure 3.65. The starting locations of the 40 molecules i1 and 40 molecules i2, randomly distributed (adapted from ref [19])

After energy minimization, the simulation was initiated and the molecules were given a time window of 800 ns for self-assembly. Upon completion of the simulations, all 80 molecules have grouped together to create a large aggregate, as can be seen in Figure 3.66.: i1-position isomer - green, i2-position isomer - red.
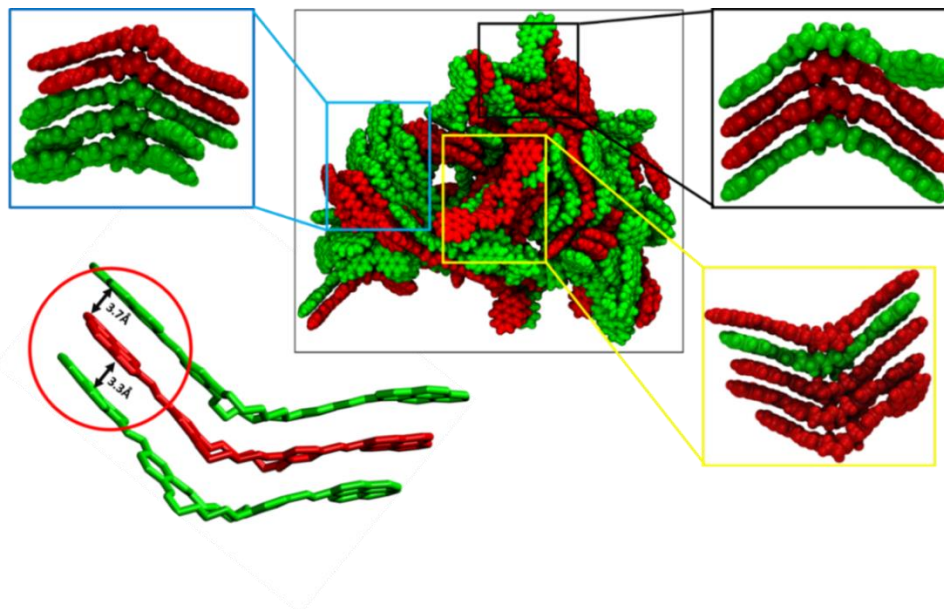
Figure 3.66. Final structure of the AzoPy-18C6 aggregate after 800 ns. The details (rotated for clarity) represent the neatly formed stacks. The red circle highlights the π - π interactions as well as the intermolecular distance between the pyrene units (adapted from ref [19])

From Figure 3.66. it can be seen that AzoPy-18C6 forms ordered stacks of 3 to 5 molecules and that these stacks aggregate with each other randomly. Furthermore, it can be seen that the position of the pyrene units does not influence the structure of the stack. The details in Figure 3.66. shows representative examples of stacks that have a mixed composition. After the simulation, no stacks composed exclusively of one of the two positional isomers (i1-i1 or i2-i2) were identified. Comparing these results with those obtained in the previous subsection regarding the study of the compound DPyDB-C=N-18C6 [13], it can be seen that the aggregate appears to have a similar basic structure as a whole. However, on closer inspection, it can be seen that there is a significant difference between the stacks that make up the aggregate (Figure 3.66).

Ground state quantum mechanical calculations

In addition to the DM simulations presented above, the intrinsic chemical and physical properties previously determined by the WAXD analysis technique and the analysis of UV-VIS and fluorescence spectra were evaluated in silico by quantum mechanical calculations. To

demonstrate the equilibrium structure and intramolecular features such as bond lengths, dihedral and valence angles, parameters that were predicted using the PBE0/6-311+G(d,p) method. The compound AzoPy-18C6 and its two isomers were evaluated in the ground state. In addition, the conformational effect of the AzoPy-18C6 molecular system, such as coplanarity or, conversely, the existence of a twisted structure, was investigated.
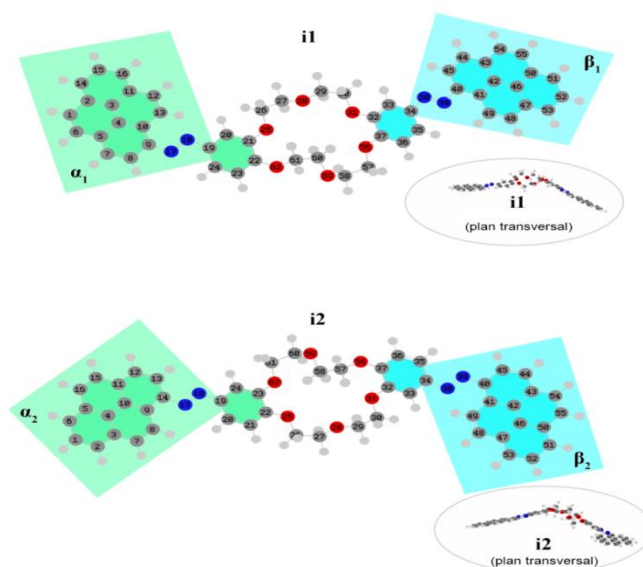
Figure 3.69. Positional isomer structures: i1 (top) and i2 (bottom), after ground-state optimization using the PBE0/6-311+G(d,p) method (adapted from ref [19])

Figure 3.69. provides a graphical representation of the geometry optimization using the chosen PBE0/6-311+G(d,p) level of theory. In this figure, the mode and plane of binding of the two pyrene units to the neighboring phenyl rings of the crown ether sequence have been marked with green and blue colors, respectively. In this mode, the isomerization modes of both i1 and i2 conformers are indicated.

Quantum mechanical calculations of excited states

To better understand the present stacking interaction process an in-depth investigation of the electron density was performed. Thus, diagrams of the gap between the frontier molecular orbitals HOMO (high energy occupied molecular orbitals) and LUMO (low energy unoccupied molecular orbitals) were made (Figure 3.70.).
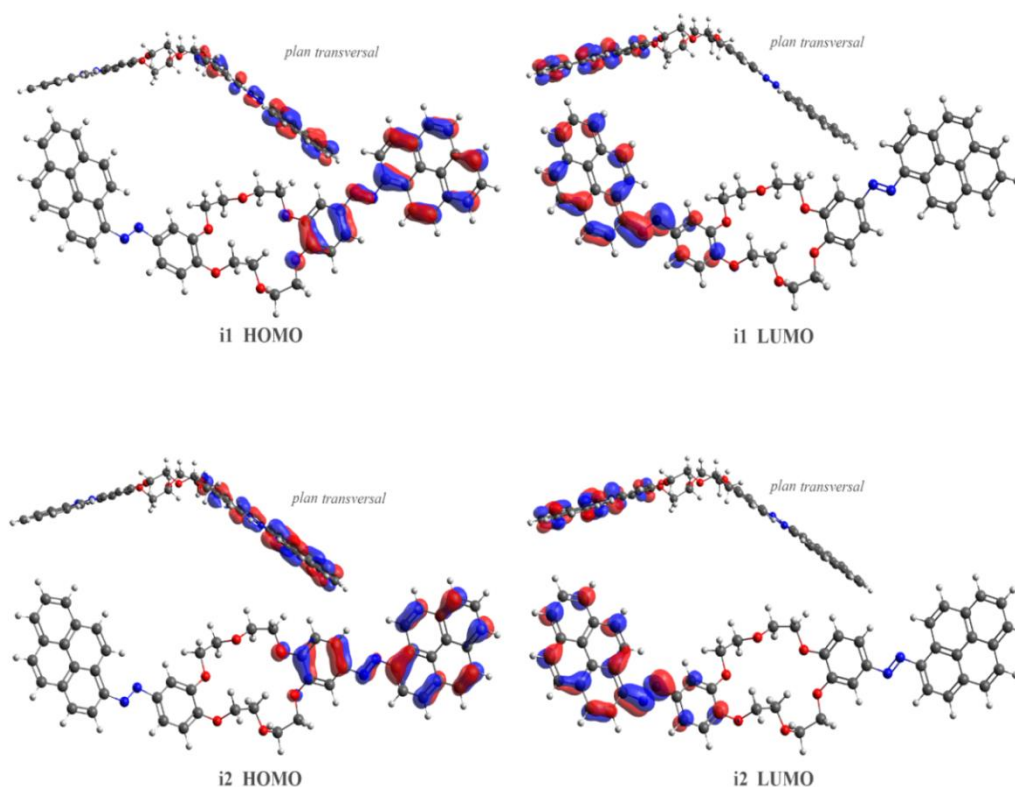
Figure 3.70. Cross-sectional view of the localized HOMO-LUMO electron densities on the i1 and i2 isomers of the azopyrene system (adapted from ref [19])

Figure 3.70. demonstrate that the electron cloud density is localized on the aromatic units (pyrene, –N=N–, phenyl) and has a π (being bonding, HOMO) and π^* (anti-bonding forming in the LUMO) type distribution. As a result of the fact that pyrene units are larger in number of atoms than phenyls and -N=N- bonds and include a large group of π bonds, the electron density was predominantly located on these sequences. Analysis of the energy difference between the HOMO and LUMO levels showed a change in the electron density of the pyrene rings as they move from the right $\beta 1$ and $\beta 2$ planar positions to the left $\alpha 1$ and $\alpha 2$ planar positions. Even if the aromatic sequences in the $\alpha 1$, $\alpha 2$, $\beta 1$ and $\beta 2$ planar positions were joined by non-conjugated chemical systems, this shift in electron density would still be visible (in the present case, the crown ether central group). Both experimental and theoretical methods validated the dimer formation of diazopyrene derivatives in the ground state. This process was shown to be governed by a weak non-covalent interaction. Figure 3.76. illustrates the non-covalent interactions that occur in each of the three possible dimer association configurations (i1-i1, i1-i2 and i2-i2).
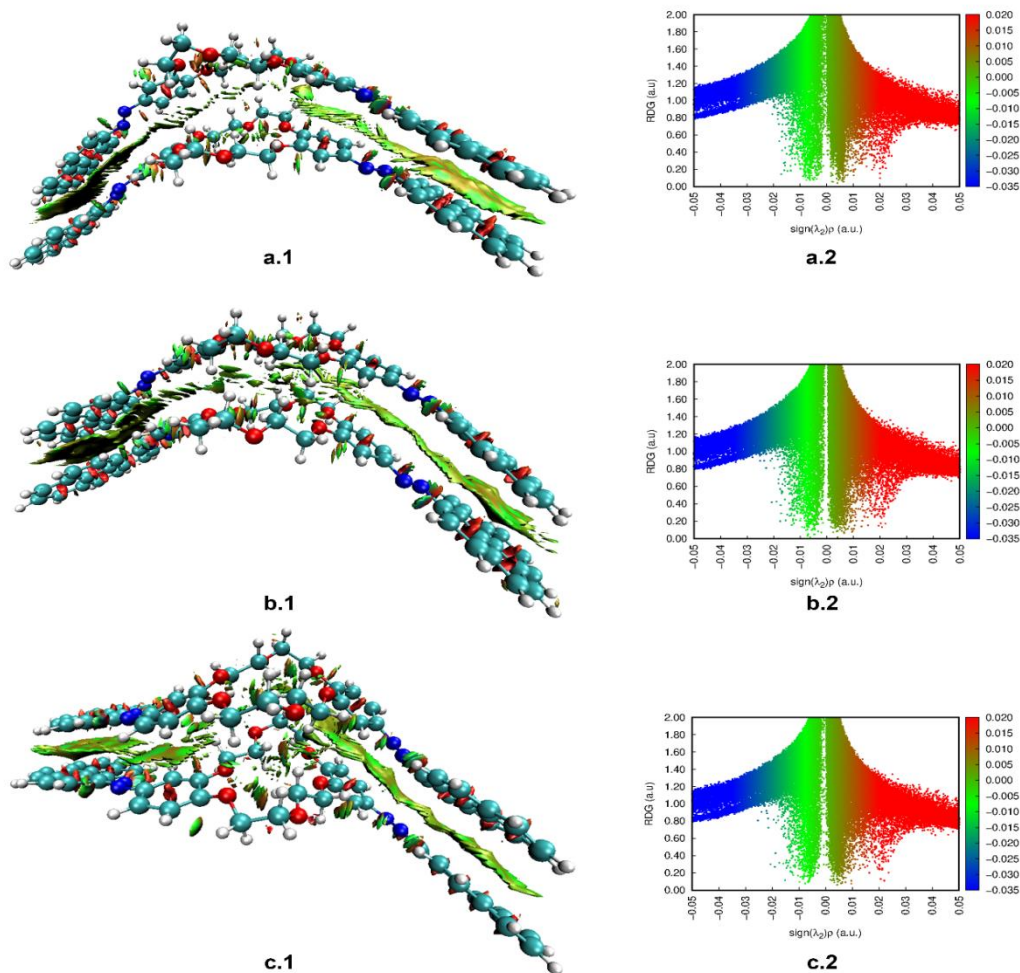
Figure 3.76. Representation of the NCI surface on the left and the NCI diagram on the right for non-covalent interactions in i1-i1 stacks (a.1, a.2); i1-i2 (b.1, b.2); i2-i2 (c.1, c.2) (adapted from ref [19])

3.3.3.4. Conclusions

❖ In this chapter, a new system was designed and obtained by linking two pyrene fragments through –N=N– bridges to each side of the crown dibenzoether. Characterization by physico-chemical techniques (FTIR, ^{1}H-NMR, ^{13}C-NMR, TGA and DSC) of the obtained compound confirmed the proposed structure.

❖ Experimentally and *in silico*, the supramolecular arrangement of the AzoPy-18C6 system has been demonstrated. DM simulations were performed to reveal the π - π stacking interactions, which were further confirmed by the WAXD analysis technique in the spectrum of which a sharp peak at 2θ of 1.914° was observed.

❖ By investigating the photophysical characteristics of the excited state using UV-Vis and fluorescence spectroscopies it was demonstrated that the aromatic pyrene fragments inside the ordered stacks of AzoPy-18C6 exhibit π - π interactions. This was further confirmed by DFT and TD-DFT calculations which showed the interaction between the electron densities of the molecular orbitals. Moreover, the presence of mixed $\pi \rightarrow \pi^*$ and n $\rightarrow \pi^*$ transitions was observed, with the $\pi \rightarrow \pi^*$ transition predominating due to the π-extended conjugation. It was also revealed by DM, DFT and TD-DFT approaches that the –N=N– bond contributed to a more planar arrangement of the molecule and an improvement in the π - π stacking ability of the molecules. At the same time, the dihedral angle in the C–N=N–C sequence, specific to azopyrene units and Van der Waals interactions, plays a key role in the π - π stacking of the AzoPy-18C6 system.

❖ The *in silico* results showed that the C-N=N-C dihedral angle, specific to azopyrene units and Van der Waals interactions, plays the dominant role in the formation of π - π aggregates and, implicitly, crown ether aggregates.

❖ DFT and TD-DFT calculations showed that the $\pi - \pi$ association is favored in the ground state and not in the excited state.

CHAPTER 4. EVALUATION OF THE POTENTIAL OF ENDOCAN AS A BIOMARKER - A FIRST STEP IN THE DESIGN OF SMART SYSTEMS FOR THE RAPID DETECTION OF ENDOCAN IN BIOLOGICAL SAMPLES

Objective: Prospective study of endocan as a biomarker in neonatal sepsis

4.1. Introduction

Early neonatal sepsis is an invasive infection that occurs in the first 72 hours of life, but in approximately 90% of cases symptoms begin within the first 24 hours after birth [20]. In the case of newborns, the clinical signs suggestive of sepsis appearing in the first 72 hours of life are non-specific, and can be attributed to other pathologies with an onset in the immediate post-natal period. On the other hand, biomarkers routinely used in the diagnosis of sepsis, such as C-reactive protein (CRP) and procalcitonin (PCT), have reduced sensitivity, specificity and positive predictive value in the first 3 days of life, being affected by multiple factors of a non-infectious nature [21].

Endocan (*endothelial cell-specific molecule-1*) is a soluble proteoglycan with a mass of 50 kDa secreted by lung and kidney endothelial cells, and is expressed in various pathologies [22,23]. In vitro experiments have shown that pro-inflammatory cytokines, such as interleukin-1β (IL-1β) and tumor necrosis factor α (TNF-α), increase the gene expression of endocan and induce its secretion by endothelial cells [24], while interferon gamma (IFNγ) inhibits it [23–27]. Endocan degradation *in vitro* under the action of serine proteases released by polymorphonuclear neutrophils has also been demonstrated [28].

Data reported in the literature have shown increased serum levels of endocan in sepsis patients, both adults and neonates, and their correlation with the severity of sepsis [24,25], reflecting endothelial activation associated with systemic inflammation. Endocan binds to leukocyte function-associated antigen (LFA-1), an integrin expressed on the surface of lymphocytes, monocytes and Jurkat cells, inhibiting its interaction with intercellular adhesion molecule 1 (ICAM-1) and thus intervening in the regulation of leukocyte migration to the site of inflammation, as well as leukocyte adhesion and activation. However, endocan also acts as a protective molecule, reducing tissue damage due to excessive leukocyte diapedesis [28–31] and could also represent a suitable biomarker for the diagnosis of sepsis.

Thus, a ***first proposed objective*** was to establish the normal values of serum endocan during the first 3 days of life in term and premature newborns without infection. We also aimed to characterize its variation at different times after birth and under the action of different factors associated with increases in inflammatory markers commonly used in practice. The ***second***

objective was to investigate the potential role of endocan in the diagnosis of early neonatal sepsis to facilitate early initiation of targeted treatment and improve the vital and long-term prognosis of neonates with sepsis.

4.2.1. Experimental design for inclusion in the study of newborns with neonatal sepsis

In collaboration with a team of neonatologists, we conducted a prospective study on newborns hospitalized in the neonatology wards of the Cuza-Vodă Obstetrics and Gynecology Clinical Hospital in Iasi. In the study we included 65 hospitalized patients in a 10-month period. Both term and preterm neonates with gestational ages (VG) between 33 and 41 weeks were recruited based on the following inclusion criteria: term or preterm neonate (with VG $\geq$ 33 weeks), on the first day of life, without risk factors for infection/clinical suspicion of sepsis, with good adaptation to extrauterine life.

The data recorded from the clinical observation sheets consisted of: gestational age (VG), birth weight (GN), sex of newborns, mode of delivery, elements of fetal distress (meconium amniotic fluid or fetal heart beat abnormalities), the need for resuscitation maneuvers at birth, APGAR score, presence of minor obstetric trauma (any of: serosanguineous bump, cephalhematoma, ecchymosis, clavicle fracture, brachial plexus elongation), risk factors for infection and clinical signs of sepsis.

The cohort included term and preterm neonates with VG between 26 and 41 weeks and postnatal age < 24 h at intensive care admission. Inclusion in the study was conditioned by the presence of the risk factors and clinical signs shown in Table 4.1. The presence of at least one risk factor and three or more clinical signs was required for inclusion in the study. Newborns with congenital anomalies were excluded from the study.

Within the study group, the newborns were divided into two groups: septic and non-septic. The septic group included neonates with confirmed infection (positive blood culture) and probable infection (clinical and laboratory data suggestive of sepsis but negative blood culture). Suspicion of infection was assessed on admission in all neonates with suggestive clinical signs. The main serum parameters considered were: C-reactive protein (CRP) and procalcitonin (PCT), and as additional serum parameters were considered: the number of white blood cells; the absolute value of polymorphonuclear neutrophils; platelet count (Table 4.2).

Table 4.1. Clinical criteria for inclusion in the study (adapted from ref [32])

Risk factors	Clinical signs	Clinical and/or biological deterioration during the first 72 h of life (considered to be due to sepsis)
Rupture of membranes > 18 h	Thermal instability	Hypotension requiring volume expander or inotropic support
Chorioamnionitis	Apnea	Anemia requiring transfusion of erythrocyte mass
Maternal fever	Supplemental oxygen required	Acidosis
Positive amniotic fluid cultures	The need for non-invasive/invasive respiratory support	Necrotic ulcerative enterocolitis
Vaginal or urinary tract infections during pregnancy	Tachycardia/bradycardia	Intraventricular hemorrhage
Lichid amniotic fetid	Digestive intolerance	

Table 4.2. Criteria used to define neonatal sepsis (adapted from ref [32])[*]

Confirmed sepsis	≥ 3 clinical signs suggestive of sepsis
	CRP ≥ 6 PCT > 0.5 ng/mL ≥ 2 modified serum parameters* Hemoculture: **positive**
Probable sepsis	**≥ 3 clinical signs suggestive of sepsis**
	CRP ≥ 6 PCT > 0.5 ng/mL ≥ 2 modified serum parameters * Hemoculture: **negative**
Possible sepsis	**< 3 clinical signs suggestive of sepsis**
	CRP < 6 PCT ≤ 0.5 ng/mL < 2 modified serum parameters * Hemoculture: **negative**
No sepsis	**Without clinical signs suggestive of sepsis**
	CRP < 6 PCT < 0.5 ng/mL No modified serum parameters ** Hemoculture: **negative**

* CRP – C reactive protein; PCT – procalcitonin. Other serum parameters: white blood cell count; the absolute value of polymorphonuclear neutrophils; platelet count.

4.2.2. Assessment of endocan levels

From each patient included in the study, 1 mL of blood was collected by peripheral venipuncture during the first 6 hours of life and then on day 3 of life. The serum endocan concentration was determined by the ELISA technique, using anti-endocan monoclonal antibodies (ELISA Kit H1, Lunginnov, Lille, France). Values were represented in ng/mL [24].

4.2.3. Statistical analysis

Statistical analysis was performed with IBM SPSS Statistics for Windows v20.0 (IBM SPSS, IBM Ireland Product Distribution Limited, Dublin, Ireland). Significant differences between groups of normally distributed variables were assessed by *Student t test* analysis (for independent or paired samples, as appropriate). The threshold for statistical significance was set at 5% (p-values less than 0.05). The Mann Whitney U test was used for the statistical analysis of non-normally distributed variables.

After processing samples from 38 term and 27 preterm neonates for whom blood samples were collected on days 1 and 3, only 39 sample pairs were validated. The rest of the samples were invalidated due to insufficient amount of serum required for ELISA analysis.

Table 4.4. Serum endocan concentration in the control group on days 1 and 3 of life (adapted from ref [33])

Serum endocan (ng/mL) mean ± SD (interval; CI 95%)	n = 22	Term	Standard error (±)	n = 17	Preterm (VG ≥ 33)	Standard error (±)	p
Day 1		1,74 ± 0,65 (0,48-3,22; CI: 1,49-2,03)	0,13		2,02 ± 0,49 (1,14-3,20; CI: 1,77-2,27)	0,11	†p = 0,11
Day 3		2,02 ± 0,48 (1,16-2,95; CI: 1,81-2,24) *p = 0,09	0,10		1,97 ± 0,74 (0,77-3,40; CI: 1,59-2,35) §p = 0,81	0,18	‡p = 0,79

SD = standard deviation; CI = confidence interval; VG = gestational age;

* significance coefficient for serum endocan between day 1 and day 3 in term neonates; §significance coefficient for serum endocan between day 1 and day 3 in preterm neonates;

†significance coefficient for day 1 serum endocan between term and preterm neonates;

‡ significance coefficient for day 3 serum endocan between term and preterm neonates.

After analyzing the results of the 39 pairs of samples, between the first and third day of life there were no statistically significant differences in the serum level of endocan (term neonates: p = 0.09, preterm: p = 0.81) (Table 4.4). There were also no statistically significant differences in serum endocan levels between term and preterm neonates, both on day 1 (p = 0.11) and day 3 (p = 0.79) of life.

Table 4.5. Variation in serum endocan concentration (ng/mL) according to mode of delivery, presence of fetal distress and minor obstetric trauma (adapted from ref [33])

	n	Day 1	p	n	Day 3	p
Caesarean ♣	31	1,76 ± 0,56	0,53	24	2,01 ± 0,79	0,42
Vaginal birth	26	1,86 ± 0,61		23	2,19 ± 0,79	
Fetal distress	8	1,76 ± 0,73	0,78	5	2,24 ± 0,19	0,67
No fetal distress	49	1,82 ± 0,56		42	2,08 ± 0,12	
Minor trauma	8	1,87 ± 0,56	0,75	6	2,17 ± 0,62	0,81
No trauma	49	1,80 ± 0,59		41	2,09 ± 0,81	

♣epidural; n – number of cases; p – p value.

4.3.2. Determination of serum endocan levels in early neonatal sepsis

The study included 59 newborns, 24 term and 35 preterm, evaluated during the first 24 hours of life for suspected sepsis, of which 32 newborns were included in the septic group, and 27 in the non-septic group (Table 4.6.).

Table 4.6. Characteristics of the newborns included in the study with neonatal sepsis, according to the severity of the sepsis (adapted from ref [32])

Lot	Gender	Gestational age		Total
		Preterm	**Term**	
Non-sepsis	Female	3	4	7
	Male	5	15	20
	Total	**8**	**19**	**27**
Sepsis	Female	5	1	6
	Male	2	2	4
	Total	**7**	**3**	**10**
Severe sepsis	Female	5	0	5
	Male	15	2	17
	Total	**20**	**2**	**22**
Total		**35**	**24**	**59**

The mean serum concentration of endocan continued to increase in both the septic and non-septic neonates, but although the mean serum level was higher in the septic neonates, the difference between the two groups was no longer statistical significance. The mean serum endocan concentration measured on day 7 was lower in patients in both groups compared to day 3, but the decrease was statistically significant only in the septic neonates (2,04 vs. 2.92, p = 0.01) (Figure 4.1.).
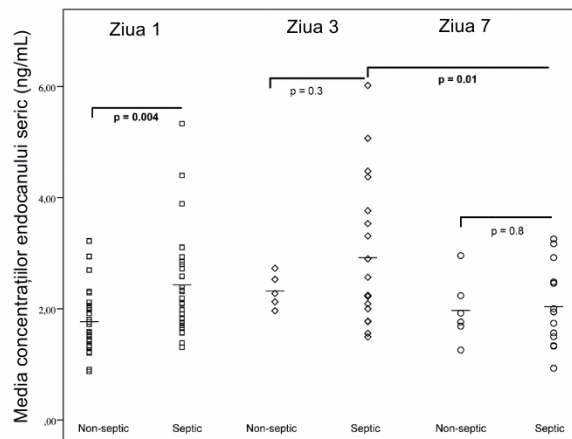
Figure 4.1. Comparison of serum endocan concentrations (ng/mL) on day 1, day 3, and day 7 in septic and non-septic neonates (adapted from ref [32]).

4.4. Conclusions

Three important conclusions can be drawn from the studies carried out in this chapter:

❖ endocan can be considered a useful marker in the diagnosis of early neonatal sepsis, as well as in monitoring the evolution under treatment;

❖ further studies should be undertaken to establish the optimal level of endocan in healthy newborns;

❖ a bionanoconjugate should be developed as a platform for ELISA assay with increased sensitivity and specificity for endocan detection. The kit available on the market for the ELISA test has a rather low sensitivity and specificity, therefore the development of bionanoconjugates as platforms for the ELISA test with high specificity in the detection of endocan from biological samples containing very small amounts of the studied analyte is required.

GENERAL CONCLUSIONS

From the results obtained from the research undertaken in the doctoral thesis *"Intelligent systems designed for the transport of active chemical species. Obtaining. Characterization"*, the following general conclusions emerge:

✓ A series of crown ether derivatives was synthesized to study their aggregation through hydrogen bonds. The chemical structures of the crown ether derivatives were confirmed by ^{1}H-NMR and HPLC-MS.

✓ The capacity to transport cations through the liposomal membrane is determined by increasing the concentration of the studied crown ether derivative.

✓ Following the analysis of EC_{50} and k, it was observed that the transport of ions through the membrane is more efficient in the case of compounds with a longer alkyl chain, consisting of the octyl and dodecyl radical compared to the compound with a shorter alkyl chain (hexyl).

✓ Differences were observed between the transport mediated by 15-crown-5 ether derivatives having octyl or dodecyl radicals in their composition depending on the transported ion. Transport of K^+ ions is faster and more efficient for the compound with the longer alkyl radical, i.e. dodecyl-benzoureido-ether-15-crown-5.

✓ By replacing the linear alkyl radical with an optically active branched one, no significant differences were observed in terms of ion transport selectivity. The transport activity of compounds with an optically active octyl radical lies between that of compounds with an n-hexyl radical and that of compounds with an n-octyl radical.

✓ For all compounds examined, the highest transport activity was recorded for K^+ and Rb^+ ions, while the lowest transport activity was observed for the ions with the smallest ionic radii, Li^+ and Na^+. This situation is evident from the Y fractional activity values and is supported by the k and EC_{50} values.

✓ During DM simulations, no phenomena of self-assembly of compounds into stable ion channels were detected. However, in Course-Grain simulations, translation of crown alkyl-benzoureido-ether molecules from one side of the lipid membrane to the other was observed. This aspect could suggest the existence of a *carrier-type transport* process. The results obtained so far indicate the presence of a complex transport mechanism.

✓ Two compounds were synthesized, by linking two pyrene fragments to diaminodibenzo-ether-18-crown-6 through bonds –HC=N–, respectively –N=N– for the study on the self-assembly of crown ether derivatives through interactions of π-π type. Obtaining the

compounds was confirmed by FTIR, ^{1}H-NMR, ^{13}C-NMR, TGA and DSC. Quantitative analysis determined by ^{13}C-NMR revealed the presence of two positional isomers for each of the two synthesized compounds.

✓ Both compounds have been shown to form supramolecular aggregates through $\pi - \pi$ interactions.

✓ The compound DPyDB-C=N-18C6 exhibits weak π-π interactions, the DM simulation results showing the existence of almost isoenergetic structures as a light-parallel aggregate with an interaction distance around 3.45 and 3.28 Å.

✓ The AzoPy-18C6 compound shows "stacks" on multiple layers, highlighted by DM simulations and confirmed by WAXD.

✓ Following the investigation of the compound DPyDB–C=N–18C6 in solvents with different polarities (n-hexane, toluene, 1,2-dichloroethane and ethanol), by UV-vis and fluorescence experiments, as well as by quantum mechanical calculations, the presence of $\pi \rightarrow \pi^*$ and $n \rightarrow \pi^*$ transitions was observed, of which the $\pi \rightarrow \pi^*$ transition due to extended π conjugation was predominant. The experiments confirmed the quantum models made for these systems.

✓ The supramolecular arrangement of the AzoPy-18C6 system has been demonstrated experimentally and by *in silico* studies.

✓ The aromatic pyrene fragments inside the ordered stacks of AzoPy-18C6 have been shown to exhibit π-π interactions following the study of the photophysical characteristics of the excited state (UV-Vis analysis and fluorescence spectroscopy). DFT and TD-DFT calculations that showed the interaction between the electron densities of the molecular orbitals confirmed the presence of mixed $\pi \rightarrow \pi^*$ and $n \rightarrow \pi^*$ transitions, with the $\pi \rightarrow \pi^*$ transition predominating due to the π-extended conjugation.

✓ It was observed that the –N=N– bond plays a key role in the π-π stacking of the AzoPy-18C6 system, by determining a planarized molecular geometry.

✓ The dihedral angle in the C–N=N–C sequence, specific to azopyrene units and Van der Waals interactions, is also important in the π-π stacking of the AzoPy-18C6 system.

✓ Following the studies carried out on term and premature newborns, based on serum endocan concentration, it was found that endocan is a biological marker with high sensitivity, but less selectivity. However, endocan can have a marker role in the process of early diagnosis in neonatal sepsis and in monitoring the response to treatment. By designing intelligent systems for endocan detection, complex systems can be developed to treat the effects of neonatal sepsis.

DISSEMINATION OF RESULTS

The scientific results presented in this doctoral thesis have so far been the subject of five scientific articles published in ISI rated journals, three participations in national scientific conferences (two oral communications and one poster) and three participations in international conferences (three posters).

I) Works published in ISI listed journals related to the doctoral thesis:

1. A. Coroaba, C. Al-Matarneh, T. Vasiliu, S.-A. Ibanescu, **R. Zonda**, I. Esanu, D.-L. Isac, M. Pinteala. Revealing the supramolecular interactions of the bis(azopyrenyl) dibenzo-18-crown-6-ether system, *Journal of Molecular Liquids*, 374, 121298, **2023**, https://doi.org/10.1016/j.molliq.2023.121298. (IF 2022 = 6)

2. A. Coroaba, D.-L. Isac, C. Al-Matarneh, T. Vasiliu, S.-A. Ibanescu, **R. Zonda**, R. Ardeleanu, A. Neamtu, D. Timpu, A. Nicolescu, F. Mocci, S. S. Maier, A. Laaksonen, M. Abadie, M. Pinteala. Probing the supramolecular features via π–π interaction of a di-iminopyrene-di-benzo-18-crown-6-ether compound: experimental and theoretical study. *RSC advances*, 10 (63), 38304-38315, **2020**, DOI: 10.1039/D0RA06929A (IF 2022 = 3.9)

3. G. I. Zonda, **R. Zonda**, A. T. Cernomaz, L. Paduraru, B. D. Grigoriu. Endocan serum concentration in uninfected newborn infants. *J. Infect. Dev. Ctries.*, 13 (9), 817-822, **2019**, https://doi.org/10.3855/jidc.11660 (IF 2022 = 2.512)

4. G. I. Zonda, **R. Zonda**, A. Cernomaz, L. Paduraru, A. Avasiloaiei, B. Grigoriu. Endocan - a potential diagnostic marker for early onset sepsis in neonates. *J. Infect. Dev. Ctries.,* 13 (4), 311-317, **2019**, https://doi.org/10.3855/jidc.11202 (IF 2022 = 2.512)

5. R. Zonda, A. Coroaba, S. Ibanescu, T. Vasiliu, A. Neamtu, M. Silion, T. Rusu, M. Pinteala. Cation transport activity of the alkyl-ureido-benzo-15-crown-5-ethers through double layer lipid membranes, *Rev. Roum. Chim.*, 63 (7-8), 665-672, **2018**, (IF 2022 = 0.5)

II) Additional works published in ISI rated journals:

1. N. Simionescu, **R. Zonda**, A. R. Petrovici, A. Georgescu. The Multifaceted Role of Extracellular Vesicles in Glioblastoma: microRNA Nanocarriers for Disease Progression and Gene Therapy, *Pharmaceutics*, 13 (7), 988, **2021**, https://doi.org/10.3390/pharmaceutics13070988 (IF 2022 = 5,4)

III) Book chapters

1. R. Zonda, S.-A. Ibanescu, M. Silion, A. Coroaba, D.-L. Isac, M. J. M. Abadie. Measuring Ionic Transport Through Lipid Bilayers. In: *New Trends in Macromolecular and Supramolecular Chemistry for Biological Applications* (eds. M. J. M. Abadie, M. Pinteala, A. Rotaru), 25-50 (Springer International Publishing), **2021**

2. M. Silion, A. Fifere, L. A. Lungoci, N. Marangoci, S.-A. Ibanescu, **R. Zonda**, A. Rotaru, M. Pinteala. Mass spectrometry as a complementary approach for noncovalently bound complexes based on cyclodextrins. In: *Advancements of Mass Spectrometry in Biomedical Research* (eds. A. G. Woods, C. C. Darie), 685–701 (Springer International Publishing), **2019**

IV) Participation in national and international scientific events

a) Oral communications:

1. R. Zonda, S. Ibanescu, A. Coroaba, T. Vasiliu, C. Al-Matarneh, M. Silion, A. Neamtu, M. Pinteala. Autoasamblarea supramoleculară a derivaților de piren prin variația mediului și a geometriei moleculare. *Zilele Academice Ieșene, a XXVII-a Sesiune de Comunicări Ştiinţifice a Institutului de Chimie Macromoleculară „Petru Poni", Progrese în ştiinţa compuşilor organici şi macromoleculari,* Iași, 2 – 4 octombrie **2019**.

2. R. Zonda, A. Coroaba, M. Silion, S. Ibanescu, M. Pinteala, M. Barboiu. Selectivity of transport capacity of the compounds based on 15-crown-5 and 18-crown-6 ethers, *Conferinţa Facultăţii de Chimie, Universitatea "Alexandru Ioan Cuza" Iași*, Iași, 27 – 28 octombrie **2016**.

b) Posters:

1. N. Simionescu, S. Nechifor, R. Buga, M. Dabija, L. Eva, **R. Zonda**, A. R. Petrovici, A. Georgescu. Microvesicle-associated microRNA signature in glioblastoma: preliminary results from OpenArray profiling. *Conferinţa Internaţională sub egida Academiei Române: cel de-al 42-lea Simpozion Aniversar al Institutului de Biologie şi Patologie Celulară "Nicolae Simionescu" şi cea de-a 38-a Sesiune Anuală a Societăţii Române de Biologie Celulară*, eveniment hibrid, București, 4 – 6 noiembrie **2021**.

2. M. Silion, C. M. Alexandrica, **R. Zonda**, A. Coroaba, S. Ibanescu, M. I. Popa. Modulation de la morphologie des Hydroxydes Doubles Lamellaires (HDL) pour la fabrication des biohybrides utilises comme vecteurs non viraux. *Dixième Colloque Franco-Roumain de Chimie Appliquée*, Bacău, 27 – 29 iunie **2018**.

3. R. Zonda, A. Coroaba, M. Silion, S. Ibanescu, M. Pinteala, M. Barboiu. Study of the transport capacity of the compounds based on modified 15-crown-5 and 18-crown-6 ethers through bilayer lipidic membranes. *18th Tetrahedron Symposium, New Developements in Organic Chemistry*, Budapest, Hungary, 27 - 30 iunie **2017**.

4. R. Zonda, A. Coroaba, S. Ibanescu, T. Vasiliu, A. Neamtu, M. Silion, M. Pinteala. Influența lungimii radicalului alchil din alchil-ureidobenzo-eteri-15-coroană-5 asupra capacității de transport cationic prin membrane lipidice dublu-strat, *Zilele Academice Ieşene, a XXVI-a Sesiune de Comunicări Ştiinţifice a Institutului de Chimie Macromoleculară „Petru Poni" Iași, Progrese în ştiinţa compuşilor organici şi macromoleculari*, Iași, 5 - 6 octombrie **2017**.

V) Trainings and courses:

1. Seminar *Electrolytes polymères pour les piles à combustible, accumulateurs lithium, cellules solaires à colorant*, dr. Cristina Iojoiu, Directeur de Recherche, CNRS, LEPMI (Laborator d'electrochimie si fisico chimie des materiales si interfate) – Grenoble - INP, Franța, organizat la Institutul de Chimie Macromoleculară „Petru Poni" Iași, 16 – 17 noiembrie **2017**.

2. *Fourth SupraChem Lab training event* organized by the ERA Chair management team, 17 – 19 septembrie **2017**.

3. *Third Suprachem Lab indoor training* organized by the ERA Chair management team, 31 mai – 01 iunie **2017**.

4. Seminar *UV/EB Curing-Principle, 3D Structures, Coatings and Thin Film Technologies*, Prof. Marc J.M. Abadie, University of Montpellier, Franța, organizat la Institutul de Chimie Macromoleculară „Petru Poni" Iași, 28 februarie – 01 martie **2017**.

5. Seminar *Auto-organized supramolecular systems by anisotropic self-assembly. Biobased polymers and matrix to develop green composites. Design of sustainable thermosets: from synthesis to properties control*, dr. Alice Cristina Mija, Associate Professor HDR at University of Nice Sophia Antipolis, Franța, organizat la Institutul de Chimie Macromoleculară „Petru Poni" Iași, 07 – 10 noiembrie **2016**.

VI) Research funding – member of research teams of national and international projects:

1. Horizon 2020 WIDESPREAD 2-2014: ERA Chairs, nr. 667387 (2016 – 2020) - Suprachem Lab - Laboratory of Supramolecular Chemistry for Adaptive Delivery Systems Era Chair Initiative. Subproject 1: Dynamic Interactive Systems for Constitutional Water and Ion Channels

2. PN-III-P4-ID-PCE-2016-0519 (2018 – 2019) – „Noi oligomeri cationici amfifili ca alternative sintetice pentru peptide antimicrobiene si/sau ca biocizi de uz extern"

REFERENCES

1. Daintith, J. Dictionary of Chemistry (6th Edition). *Oxford Univ. Press* **2008**, doi:10.1016/B978-0-08-011600-6.50016-4.
2. Gokel, G.W.; Leevy, W.M.; Weber, M.E. Crown Ethers: Sensors for Ions and Molecular Scaffolds for Materials and Biological Models. *Chem. Rev.* **2004**, *104*, 2723–2750, doi:10.1021/cr020080k.
3. Steed, J.W. First- and Second-Sphere Coordination Chemistry of Alkali Metal Crown Ether Complexes. *Coord. Chem. Rev.* **2001**, *215*, 171–221, doi:10.1016/S0010-8545(01)00317-4.
4. Sakai, N.; Matile, S. Synthetic Ion Channels. *Langmuir* **2013**, *29*, 9031–9040, doi:10.1021/la400716c.
5. Sanders, J.K. *Supramolecular Chemistry. Concepts and Perspectives. VonJ.-M. Lehn. VCH Verlagsgesellschaft, Weinheim, 1995. 271 S., Geb. 128.00 DM/Broschur 58.00 DM. - ISBN 3-527-29312-4/3-527-29311-6*; 1995; Vol. 107; ISBN 3527293116.
6. Cazacu, A.; Tong, C.; Van Der Lee, A.; Fyles, T.M.; Barboiu, M. Columnar Self-Assembled Ureido Crown Ethers: An Example of Ion-Channel Organization in Lipid Bilayers. *J. Am. Chem. Soc.* **2006**, *128*, 9541–9548, doi:10.1021/ja061861w.
7. Barboiu, M.; Vaughan, G.; Van Der Lee, A. Self-Organized Heteroditopic Macrocyclic Superstructures. *Org. Lett.* **2003**, *5*, 3073–3076, doi:10.1021/ol035096r.
8. Gilles, A.; Barboiu, M. Highly Selective Artificial K+ Channels: An Example of Selectivity-Induced Transmembrane Potential. *J. Am. Chem. Soc.* **2016**, *138*, 426–432.
9. Zonda, R.; Coroaba, A.; Ibanescu, S.; Vasiliu, T.; Neamtu, A.; Silion, M.; Rusu, T.; Pinteala, M. Cation Transport Activity of the Alkyl-Ureido-Benzo-15-Crown-5-Ethers through Double Layer Lipid Membranes. *Rev. Roum. Chim.* **2018**, *63*, 665–672.
10. Pinteala, M.; Epure, V.; Harabagiu, V.; Simionescu, B.C.; Schlick, S. Concentration- and PH-Dependent Conformational Changes and Aggregation of Block Copolymers of Poly(Methacrylic Acid) and Poly(Dimethylsiloxane) in Aqueous Media, Based on Fluorescence Spectra of Pyrene and Potentiometry. *Macromolecules* **2004**, *37*, 4623–4634, doi:10.1021/MA0496697/ASSET/IMAGES/LARGE/MA0496697F00010.JPEG.
11. Szajdzinska-Pietek, E.; Pinteala, M.; Schlick, S. Monitoring PH-Dependent Conformational Changes in Aqueous Solutions of Poly(Methacrylic Acid)-b-Polydimethylsiloxane Copolymer Based on Fluorescence Spectra of Pyrene and 1,3-Bis(1-Pyrenyl)Propane. *Polymer (Guildf).* **2004**, *45*, 4113–4120.
12. Hoche, J.; Schmitt, H.-C.C.; Humeniuk, A.; Fischer, I.; Mitrić, R.; Röhr, M.I.S.S. The Mechanism of Excimer Formation: An Experimental and Theoretical Study on the Pyrene Dimer. *Phys. Chem. Chem. Phys.* **2017**, *19*, 25002–25015, doi:10.1039/C7CP03990E.
13. Coroaba, A.; Isac, D.L.; Al-Matarneh, C.; Vasiliu, T.; Ibanescu, S.A.; Zonda, R.; Ardeleanu, R.; Neamtu, A.; Timpu, D.; Nicolescu, A.; et al. Probing the Supramolecular Features: Via π-π Interaction of a Di-Iminopyrene-Di-Benzo-18-Crown-6-Ether Compound: Experimental and Theoretical Study. *RSC Adv.* **2020**, *10*, 38304–38315, doi:10.1039/d0ra06929a.
14. Ardeleanu, R.; Voiculescu, N.; Marcu, M.; Roman, G.; Buchidau, C.; Sacarescu, L.; Sacarescu, G.; Ghica, G.; Alley, V. Synthesis of a New Siloxane-Crown Ether Polyamide P-. **1997**, *746*, 739–746.
15. Deo, C.; Bogliotti, N.; Métivier, R.; Retailleau, P.; Xie, J. Photoswitchable Arene Ruthenium Complexes Containing O-Sulfonamide Azobenzene Ligands. *Organometallics* **2015**, *34*, 5775–5784, doi:10.1021/ACS.ORGANOMET.5B00871/SUPPL_FILE/OM5B00871_SI_003.CIF.
16. Al Matarneh, C.; Ciobanu, C.I.; Mangalagiu, V.; Zbancioc, G.; Danac, R. Microwave Assisted Synthesis of Six Member Ring Azaheterocycles and Their Antimycobacterial and Anticancer Evaluation. *Rev. Chim.* **2020**, *71*, 287–293, doi:10.37358/RC.20.3.7999.
17. Al Matarneh, C.M.; Ciobanu, C.I.; Apostu, M.O.; Mangalagiu, I.I.; Danac, R. Cycloaddition versus Amidation in Reactions of 2-Amino-2-Oxoethyl-Phenanthrolinium Ylides to Activated Alkynes and Alkenes. *Comptes Rendus Chim.* **2018**, *21*, 1–8, doi:10.1016/J.CRCI.2017.11.003.
18. Al Matarneh, C.M.; Apostu, M.O.; Mangalagiu, I.I.; Danac, R. Reactions of Ethyl Cyanoformate with Cycloimmonium Salts: A Direct Pathway to Fused or Substituted Azaheterocycles.

Tetrahedron **2016**, *72*, 4230–4238, doi:10.1016/J.TET.2016.05.061.

19. Coroaba, A.; Al-Matarneh, C.; Vasiliu, T.; Ibanescu, S.-A.; Zonda, R.; Esanu, I.; Isac, D.-L.; Pinteala, M. Revealing the Supramolecular Interactions of the Bis(Azopyrenyl) Dibenzo-18-Crown-6-Ether System. *J. Mol. Liq.* **2023**, *374*, 121298, doi:10.1016/J.MOLLIQ.2023.121298.

20. Plano, L.R.W. The Changing Spectrum of Neonatal Infectious Disease. *J. Perinatol.* **2010**, *30*, S16-20, doi:10.1038/jp.2010.92.

21. Sucilathangam, G.; Amuthavalli, K.; Velvizhi, G.; Ashihabegum, M.; Jeyamurugan, T.; Palaniappan, N. Early Diagnostic Markers for Neonatal Sepsis: Comparing Procalcitonin (PCT) and C-Reactive Protein (CRP). *J. Clin. diagnostic Res.* **2012**, 627–631.

22. Lassalle, P.; Molet, S.; Janin, A.; Van der Heyden, J.; Tavernier, J.; Fiers, W.; Devos, R.; Tonnel, A.B. ESM-1 Is a Novel Human Endothelial Cell-Specific Molecule Expressed in Lung and Regulated by Cytokines. *J. Biol. Chem.* **1996**, *271*, 20458–20464, doi:10.1074/jbc.271.34.20458.

23. Bechard, D.; Meignin, V.; Scherpereel, A.; Oudin, S.; Kervoaze, G.; Bertheau, P.; Janin, A.; Tonnel, A.B.; Lassalle, P. Characterization of the Secreted Form of Endothelial-Cell-Specific Molecule 1 by Specific Monoclonal Antibodies. *J. Vasc. Res.* **2000**, *37*, 417–425, doi:10.1159/000025758.

24. Scherpereel, A.; Depontieu, F.; Grigoriu, B.; Cavestri, B.; Tsicopoulos, A.; Gentina, T.; Jourdain, M.; Pugin, J.; Tonnel, A.B.; Lassalle, P. Endocan, a New Endothelial Marker in Human Sepsis. *Crit. Care Med.* **2006**, *34*, 532–537, doi:10.1097/01.CCM.0000198525.82124.74.

25. Saldir, M.; Tunc, T.; Cekmez, F.; Cetinkaya, M.; Kalayci, T.; Fidanci, K.; Babacan, O.; Erdem, G.; Kocak, N.; Sari, E.; et al. Endocan and Soluble Triggering Receptor Expressed on Myeloid Cells-1 as Novel Markers for Neonatal Sepsis. *Pediatr. Neonatol.* **2015**, *56*, 415–421, doi:10.1016/j.pedneo.2015.03.006.

26. Buhimschi, I.A.; Buhimschi, C.S. The Role of Proteomics in the Diagnosis of Chorioamnionitis and Early-Onset Neonatal Sepsis. *Clin. Perinatol.* 2010, *37*, 355–374.

27. Simonsen, K.A.; Anderson-Berry, A.L.; Delair, S.F.; Dele Davies, H. Early-Onset Neonatal Sepsis. *Clin. Microbiol. Rev.* **2014**, *27*, 21–47, doi:10.1128/CMR.00031-13.

28. Palud, A.; Parmentier-Decrucq, E.; Pastre, J.; De Freitas Caires, N.; Lassalle, P.; Mathieu, D. Evaluation of Endothelial Biomarkers as Predictors of Organ Failures in Septic Shock Patients. *Cytokine* **2015**, *73*, 213–218, doi:10.1016/j.cyto.2015.02.013.

29. Pauly, D.; Hamed, S.; Behnes, M.; Lepiorz, D.; Lang, S.; Akin, I.; Borggrefe, M.; Bertsch, T.; Hoffmann, U. Endothelial Cell-Specific Molecule–1/Endocan: Diagnostic and Prognostic Value in Patients Suffering from Severe Sepsis and Septic Shock. *J. Crit. Care* **2016**, *31*, 68–75, doi:10.1016/j.jcrc.2015.09.019.

30. Béchard, D.; Scherpereel, A.; Hammad, H.; Gentina, T.; Tsicopoulos, A.; Aumercier, M.; Pestel, J.; Dessaint, J.-P.; Tonnel, A.-B.; Lassalle, P. Human Endothelial-Cell Specific Molecule-1 Binds Directly to the Integrin CD11a/CD18 (LFA-1) and Blocks Binding to Intercellular Adhesion Molecule-1. *J. Immunol.* **2001**, *167*, 3099–3106, doi:10.4049/jimmunol.167.6.3099.

31. Buyuktiryaki, M.; Tayman, C.; Okur, N.; Serkant, U.; Cakir, U.; Halil, H.; Oncel, M.Y.; Oguz, S.S. Can Endocan Predict Late-Onset Neonatal Sepsis? *J. Pediatr. Infect. Dis.* **2019**, *14*, 96–102, doi:10.1055/s-0038-1675239.

32. Zonda, G.I.; Zonda, R.; Cernomaz, A.T.; Păduraru, L.; Avasiloaiei, A.L.; Grigoriu, B.D. Endocan - A Potential Diagnostic Marker for Early Onset Sepsis in Neonates. *J. Infect. Dev. Ctries.* **2019**, *13*, 311–317, doi:10.3855/jidc.11202.

33. Zonda, G.I.; Zonda, R.; Cernomaz, A.T.; Paduraru, L.; Grigoriu, B.D. Endocan Serum Concentration in Uninfected Newborn Infants. *J. Infect. Dev. Ctries.* **2019**, *13*, 817–822, doi:10.3855/jidc.11660.